Experimental Activities in Berkeley

Andrew S. Voyles

14 November 2016

Nuclear Data Week 2016 - CSEWG

Berkeley
UNIVERSITY OF CALIFORNIA

Overview

- Berkeley is currently leading a targeted experimental campaign to address these needs:
  - (n,p) production cross sections – UCB
  - Stacked-target charged particle excitation functions - LBNL
  - Tunable broad-spectrum neutron source – LBNL
- Nuclear structure
  - ^{56}Fe level scheme / lifetimes – GRETINA @ ANL

^{64}Cu and ^{47}Sc (n,p) Cross-Section Measurements for Medical Radionuclide Production

UCB

Some perspective

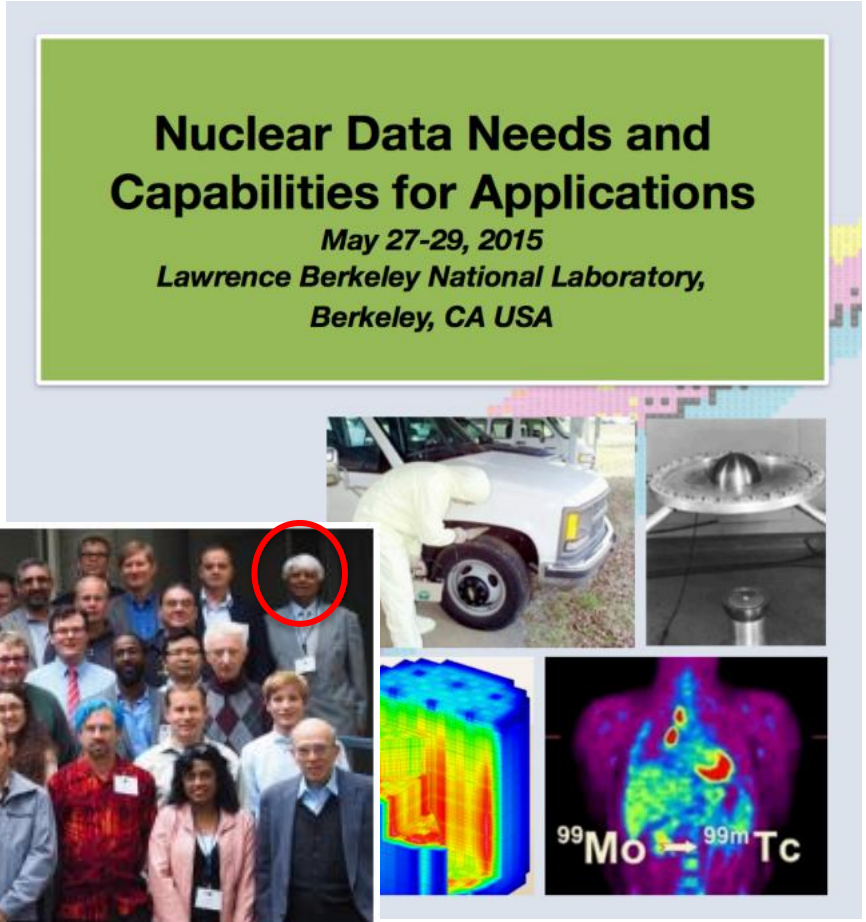

Some perspective

Isotope Production Needs

1. Charged-particle reactions for the production of medical isotopes at low energies (E < 30 MeV):
   - $^{45}Sc(p,n)^{45}Ti$; $^{52}Cr(p,n)^{52}Mn$; $^{54}Fe(d,n)^{55}Co$; $^{67}Zn(p,\alpha)^{64}Cu$; $^{72}Ge(p,n)^{72}As$, $^{74}Se(d,n)^{75}Br$; $^{86}Sr(p,n)^{86}Y$; $^{120}Te(p,n)^{120}I$

2. 100

   - $^{59}Co(p,3n)^{57}Ni$, $^{75}As(p,3n)^{73}Se$, ^{8}
     $^{121}Sb(p,3n)^{119}Te/^{119}Sb$, $^{133}Cs(p,3$
   - $^{55}Mn(p,4n)^{52}Fe$, $^{71}Ga(p,4n)^{68}Ge$,
   - $^{133}Cs(p,5n)^{128}Ba$
   - $^{127}I(p,6n)^{122}Xe$
   - $^{nat}Br(p,x)^{72}Se$, $^{nat}In(p,x)^{110}Sn$, ^{122}T
   - $^{nat}Sb(p,xn)^{119}Te/^{119}Sb$, $^{nat}La(p,xn$
   - $^{68}Zn(p,\alpha n)^{64}Cu$
   - $^{68}Zn(p,2p)^{67}Cu$, $^{124}Xe(p,2p)^{123}I$
   - $^{124}Xe(p,pn)^{123}Xe$
   - (p,x) reaction on $^{94-98}Mo$ for imp
   - $^{107}Ag(p,\alpha n)^{103}Pd$
   - $^{116}Cd(\alpha,3n)^{117m}Sn$; $^{192}Os(\alpha,3n)^{193}$

3. Nuclear data needed for radionuclides fission neutrons:
   - $^{36}S(n,x)^{32}Si$
   - $^{nat}Cl(n,x)^{32}Si$, $^{37}Cl(n,x)^{32}Si$
   - $^{nat}Zn(n,x)^{67}Cu$, $^{68}Zn(n,x)^{67}Cu$, ^{70}Z
   - $^{226}Ra(n,2n)^{225}Ra$
   - $^{232}Th(n,x)^{225}Ac$, $^{232}Th(n,x)^{227}Ac$
   - $^{32}S(n,p)^{32}P$; $^{47}Ti(n,p)^{47}Ca$, $^{64}Zn(n,$
     $^{149}Sm(n,p)^{149}Pm$, $^{153}Eu(n,p)^{153}Sm$
     $^{169}Tm(n,p)^{169}Er$; $^{175}Lu(n,p)^{175}Yb$;

4. High-energy photon-induced reactions
   - $^{68}Zn(\gamma,p)^{67}Cu$; $^{100}Mo(\gamma,n)^{99}Mo$; ^{10}

5. Nuclear da
   - 100
   - 232
   - $^{100}Mo(d,p2n)$
   - $^{100}Mo(n,2n)$
   - $^{100}Mo(p,pn)$ - data on long-lived

7. Nuclear data needed for Super Heavy Element (SHE) target
   - $^{248}Cm(n,\gamma)$ low energy resonances
   - $^{249}Bk(n,\gamma)$

$^{32}S(n,p)^{32}P$; $^{47}Ti(n,p)^{47}Ca$, $^{64}Zn(n,p)^{64}Cu$; $^{67}Zn(n,p)^{67}Cu$; $^{89}Y(n,p)^{89}Sr$, $^{105}Pd(n,p)^{105}Rh$; $^{149}Sm(n,p)^{149}Pm$, $^{153}Eu(n,p)^{153}Sm$, $^{159}Tb(n,p)^{159}Gd$; $^{161}Dy(n,p)^{161}Tb$; $^{166}Er(n,p)^{166}Ho$; $^{169}Tm(n,p)^{169}Er$; $^{175}Lu(n,p)^{175}Yb$; $^{177}Hf(n,p)^{177}Lu$

Gamma yield spectrum for incident neutron energies in the heat generation rates:
   - *Te(n,γ) (production of ^{131}I)
   - *Mo(n,γ)
   - *Ru(n,γ)
   - $^{103}Rh(n,\gamma)$
   - $^{154}Eu(n,\gamma)$
   - $^{155}Eu(n,\gamma)$
   - $^{141}Ce(n,\gamma)$
   - $^{140}Ce(n,\gamma)$
   - *Sn(n,γ)

Note: * indicates stable isotopes

Excitation function for incident neutron energies from therm
   - $^{177}Lu(n,\gamma)$, $^{154}Eu(n,\gamma)$, $^{155}Eu(n,\gamma)$, $^{77}As(n,\gamma)$, $^{72}As(n,\gamma)$,

1. $^{117}Sn(n,n')$, covering energy response 0.3 – 3.0 MeV
2. Data to support new evaluations
   - $^{23}Na(n,\gamma)$, discrepant in fast neutron region, > 100 ke
   - $^{23}Na(n,2n)$
   - $^{27}Al(n,2n)$
3. Address discrepancies:

4. Need small uncertainties on all dosimetry reactions

n standard benchmark neutron field
, $^{31}P(n,p)$, $^{10}B(n,X)\alpha$, $^{54}Fe(n,\alpha)$, $^{23}Na(n,2n)$, $^{186}W(n,\gamma)$,
Sc(n,γ), and $^{64}Zn(n,p)$
ary
n,f) and $^{238}U(n,2n)$

6. IRMM Exploratory Study of Validation Data in ^{252}Cf Standard Neutron Benchmark Field
   - Issues with existing $^{197}Au(n,\gamma)$ due to room return
   - Issues with existing $^{90}Zr(n,2n)$ due to Th contamination
   - Issue with existing $^{96}Zr(n,2n)$ due to $^{94}Zr(n,\gamma)$ contribution

^{9}Tc and $^{nat}Mo(\alpha, X)^{97}Ru$

8. Validation data in 30 keV MAC
   $^{238}U(n,\gamma)$
9. Test and improve decay chara

Inertial Confinement Fusion Data Needs

1. Accurate, temperature-dependent fusion reactivity for light ions is of primary importance to describe thermonuclear burn.
   - d(t,α)n, t(t, α)2n, d(d,t)p, d(d,^{3}He)n, d(^{3}He, α)p

4. Need small uncertainties on all dosimetry reactions

   - Xe dopants to probe ablation front instabilities.
   - Br(d,2n)Kr to probe ablator/cold fuel and ablator/hot core mix.
   - Alpha particle induced reactions to probe hot core mix: ^{6}Li, ^{9}Be, ^{10}B (best one), ^{12}C, ^{14}N, ^{16}O, ^{19}F, ^{20}Ne, ^{23}Na, ^{24}Mg, ^{27}Al.

10. Gamma Emission Probabilities
    - ^{103m}Rh -- X-ray emissi
    - ^{56}Fe, ^{54}Fe (ASTM E693
12. Uncertainty in recoil spectrum
    - Recoil spectrum chara
    - ^{69}Ga, ^{71}Ga, ^{75}As
    - Fe isotopes
    - Validate/test use of ca

4. Gamma-ray diagnostics for performance and ablator/fuel instabilities.
   - Total yield from d-t fusion γ branching ratio at 17.6 MeV.
   - $^{12}C(n,n'\gamma)$ 4.4 MeV time-integrated emission provides hydrocarbon areal densities (remaining mass). Cross section at 14 MeV must be accurate.
   - Does $^{13}C(n,n'\gamma)$ have strong emission near 4 MeV? If not, then a useful mix diagnostic is possible.
5. Solid Radiochemistry Diagnostic (SRC) is currently an NIF diagnostic complementary to ^{12}C-γ GRH detection (CH ρr).
   - Ratio of $^{198}Au/^{196}Au$ from the activated hohlraum.
   - (n,γ)/(n,2n):low energy neutrons/14 MeV neutrons.

Highlight from WTTC 2016: $^{54}Fe(p,\alpha)^{51}Mn$

NDNCA Whitepaper available at http://bang.berkeley.edu/events/ndnca/whitepaper/

Berkele
UNIVERSITY OF CALIFORNIA

Medical Applications

- Emerging medical radionuclides
  - ^{64}Cu ($t_{1/2}$ = 12.7 hr) – 61% β^+ to ^{64}Ni, 39% β^- to ^{64}Zn
  - ^{47}Sc ($t_{1/2}$ = 3.35 d) – β^- to ^{47}Ti, with 159-keV γ

Promising Prospects for ^{44}Sc-/^{47}Sc-Based Theragnostics: Application of ^{47}Sc for Radionuclide Tumor Therapy in Mice

Cristina Müller[1], Maruta Bunka[2,3], Stephanie Haller[1], Ulli Köster[4], Viola Groehn[5], Peter Bernhardt[6,7], Nicholas van der Meulen[2], Andreas Türler[2,3], and Roger Schibli[1,8]

[1]Center for Radiopharmaceutical Sciences ETH-PSI-USZ, Paul Scherrer Institute, Villigen-PSI, Switzerland; [2]Laboratory of Radiochemistry and Environmental Chemistry, Paul Scherrer Institute, Villigen-PSI, Switzerland; [3]Laboratory of Radiochemistry and Environmental Chemistry, Department of Chemistry and Biochemistry University of Bern, Bern, Switzerland; [4]Institut Laue-Langevin, Grenoble, France; [5]Merck and Cie, Schaffhausen, Switzerland; [6]Department of Radiation Physics, The Sahlgrenska Academy, University of Gothenburg, Gothenburg, Sweden; [7]Department of Medical Physics and Medical Bioengeneeri University Hospital, Gothenburg, Sweden; and [8]Department of Chemistry and Applied Biosciences, ETH Zuric

In Vivo Evaluation of Pretargeted ^{64}Cu for Tumor Imaging and Therapy

Michael R. Lewis, PhD[1]; Mu Wang, MD[1]; Donald B. Axworthy, BS[2]; Louis J. Theodore, PhD[2]; Robert W. Mallet, BS[2]; Alan R. Fritzberg, PhD[2]; Michael J. Welch, PhD[1]; and Carolyn J. Anderson, PhD[1]

[1]Mallinckrodt Institute of Radiology, Washington University School of Medicine, St. Louis, Missouri; and [2]NeoRx Corporation, Seattle, Washington

The UC Berkeley High Flux Neutron Generator

2.45 MeV neutrons, 10^8 n/s/cm^2
Extraction Plate: 5mm diameter

Commissioning:
25 July 2015

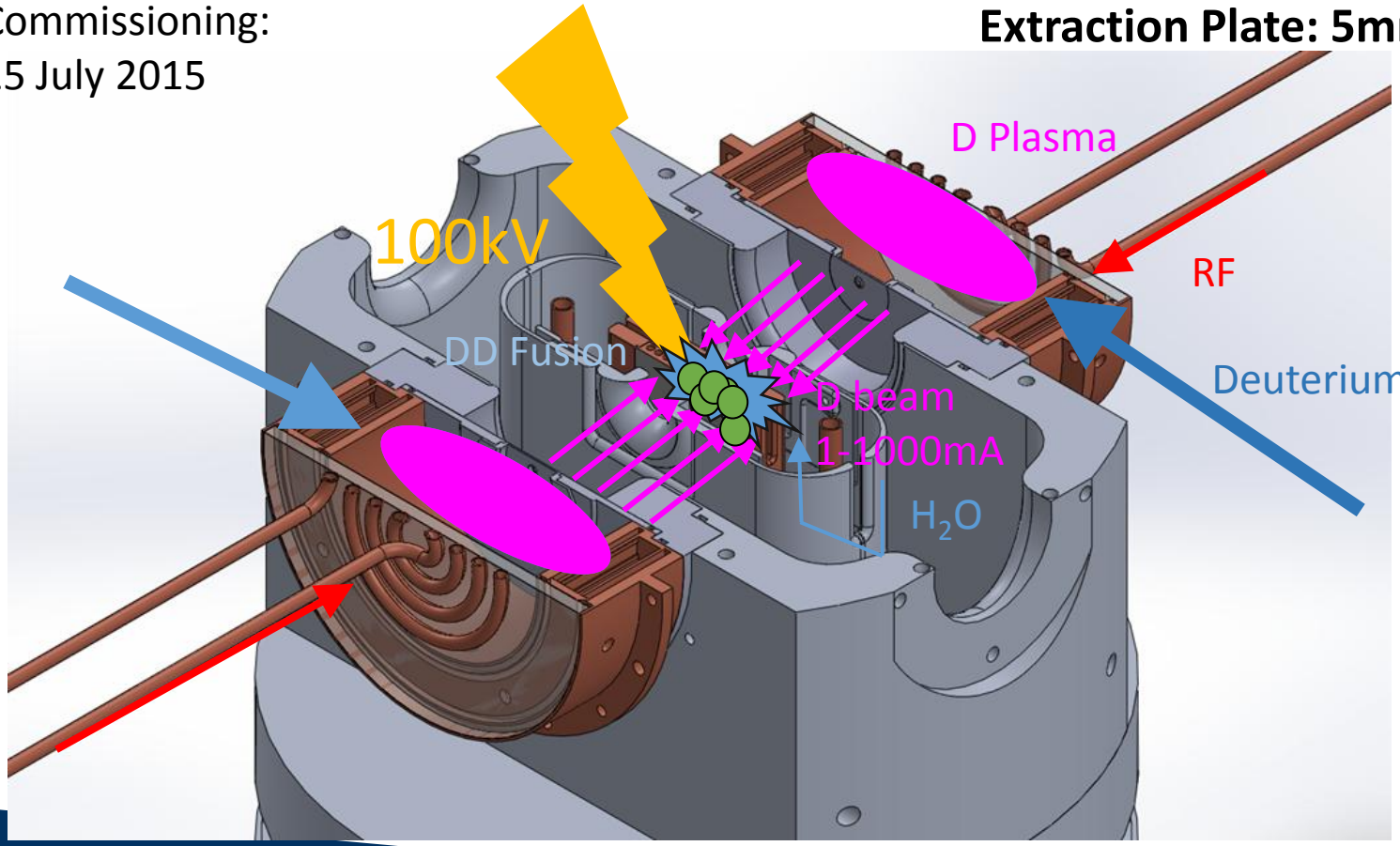

The UC Berkeley High Flux Neutron Generator

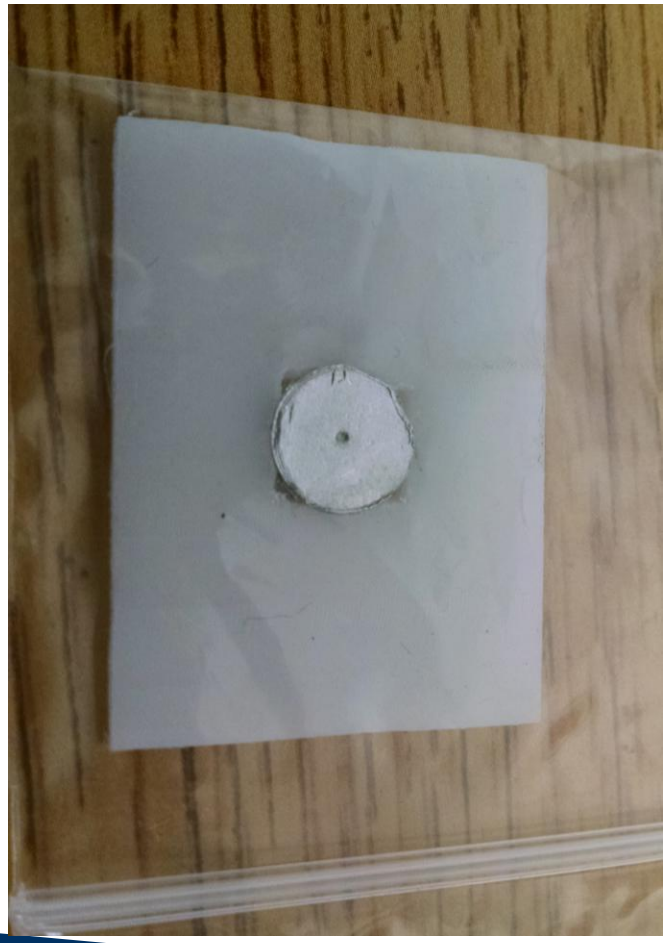

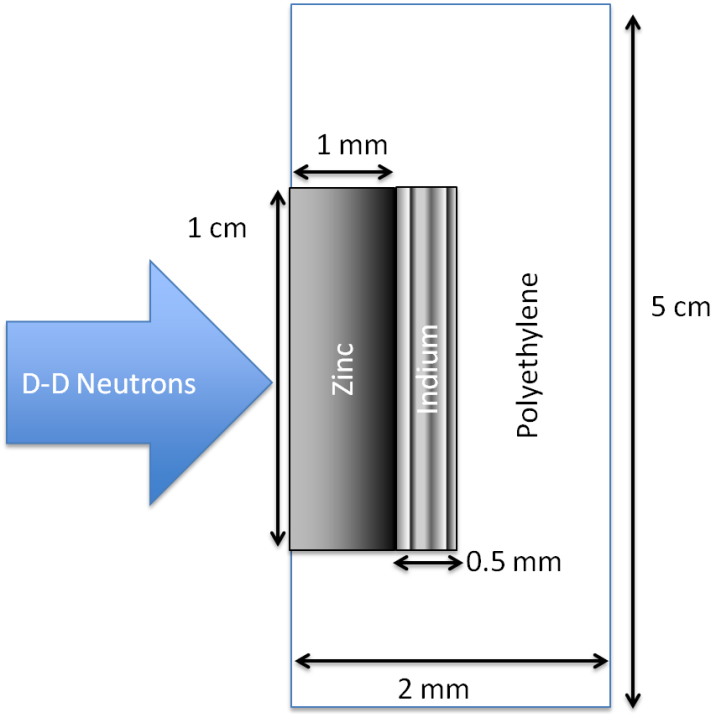

Foils Used	Metal Purity	Abundance (a/o)	Foil Density (mg/cm^2)
^{nat}In	> 99.999%	^{113}In (4.29%), ^{115}In (95.71%)	365.5
^{nat}Zn	> 99.99%	^{64}Zn (49.17%)	714.1
^{nat}Ti	99.999%	^{47}Ti (7.44%)	450.6

The UC Berkeley High Flux Neutron Generator

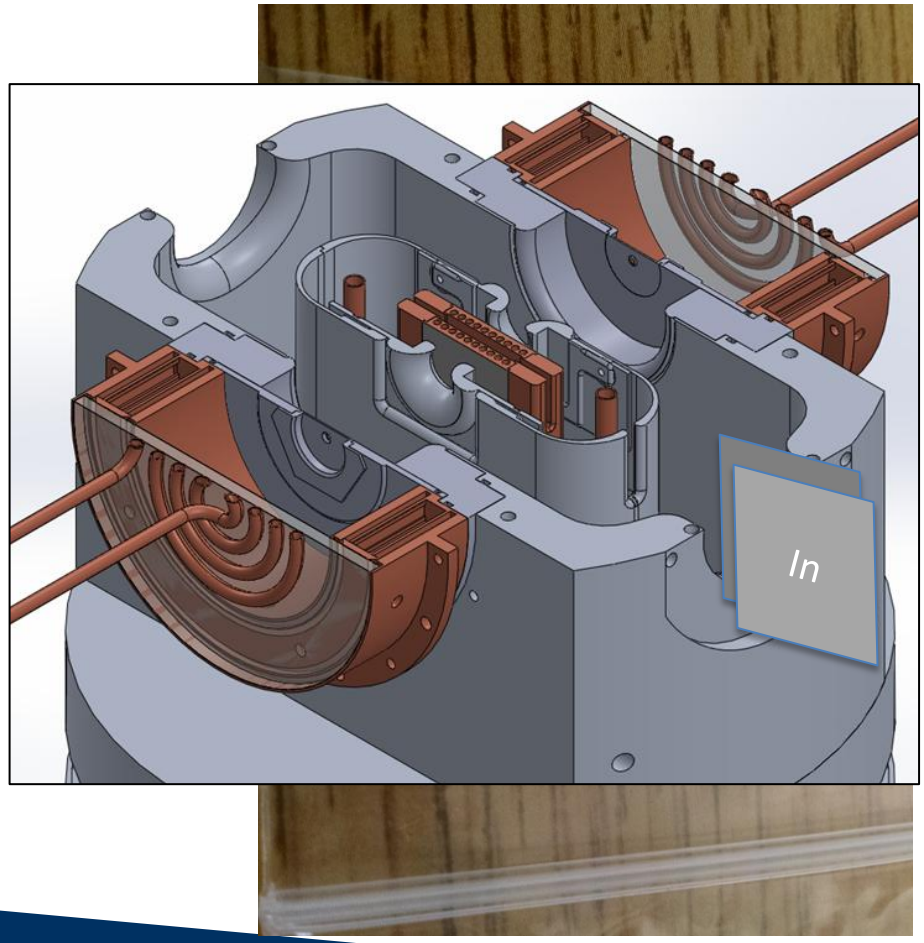

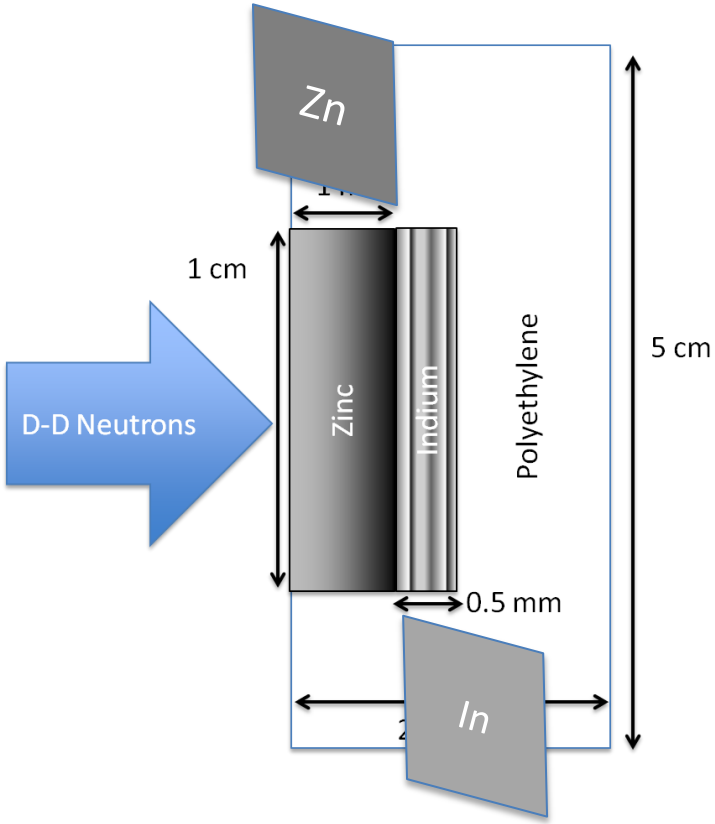

The UC Berkeley High Flux Neutron Generator

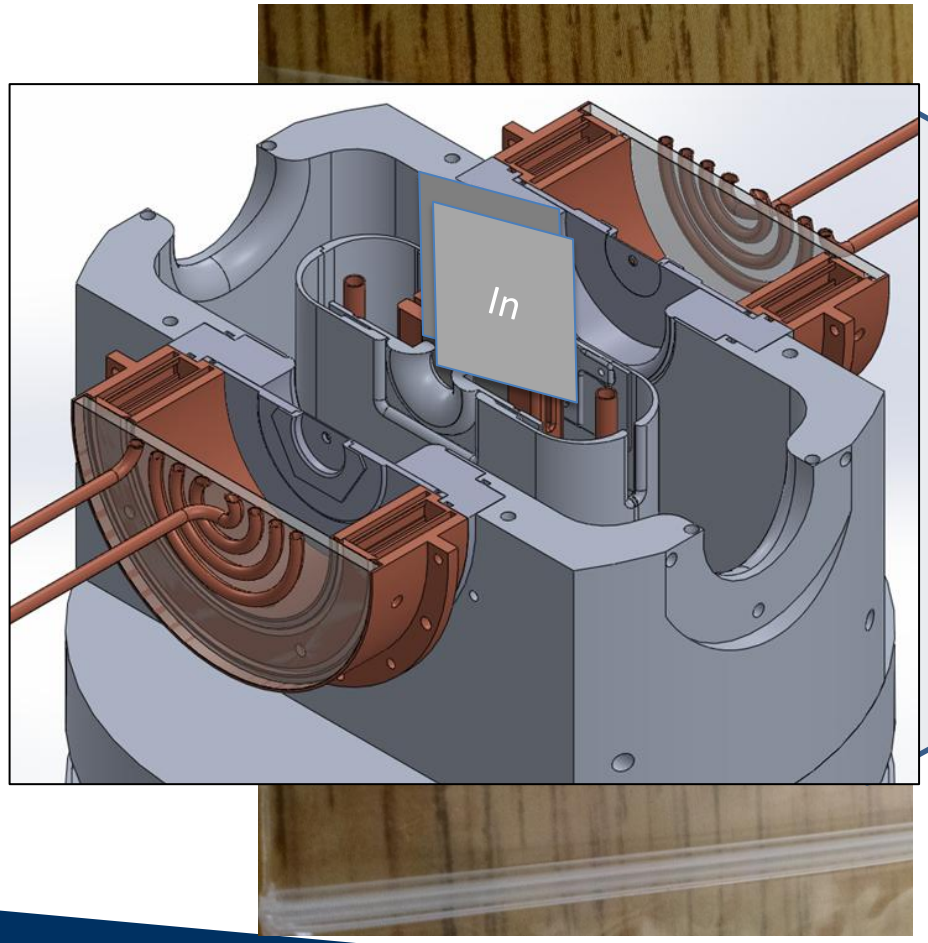

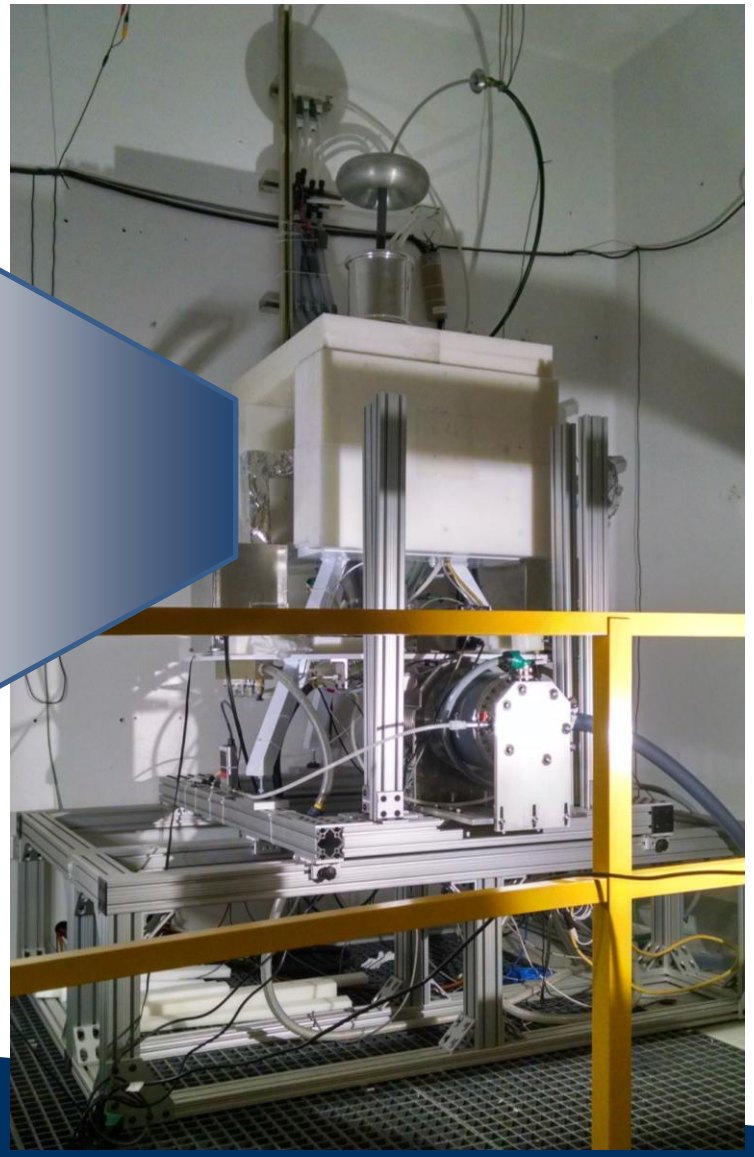

Relative Activation Measurements

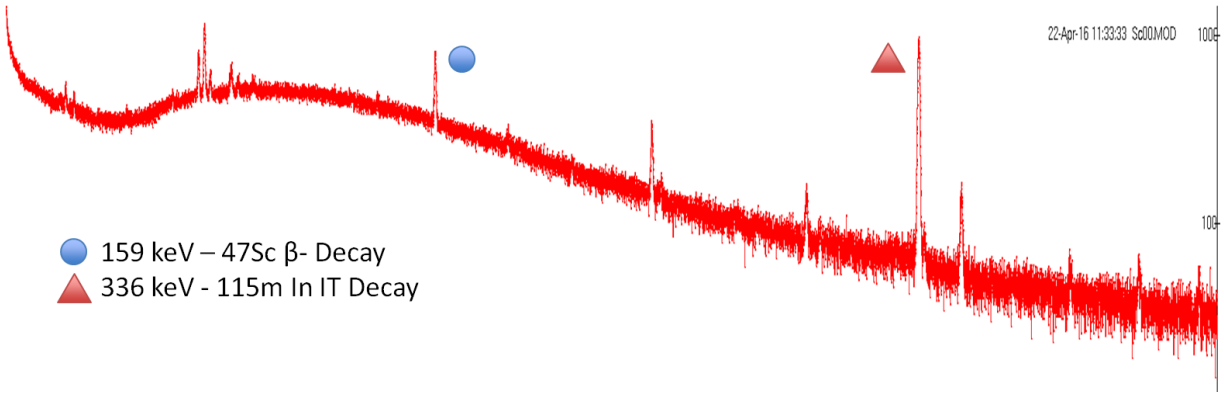

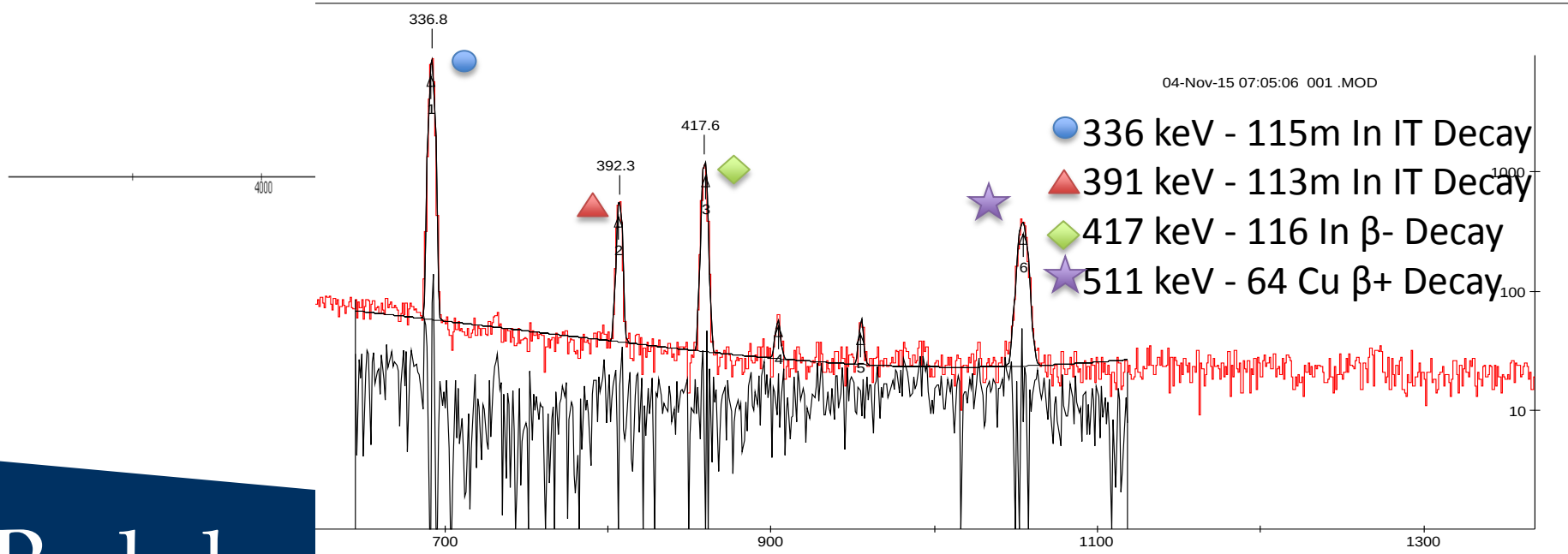

Relative Activation Measurements

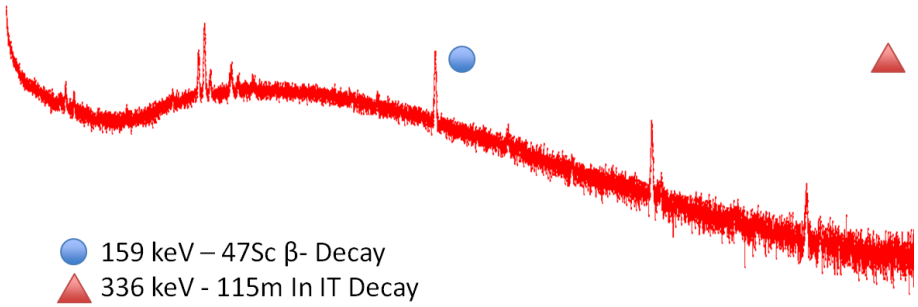

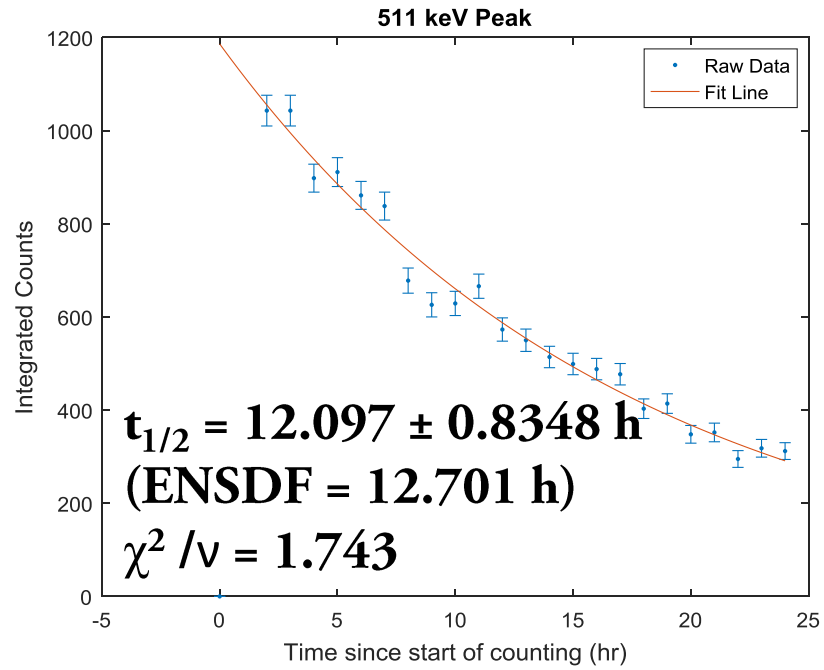

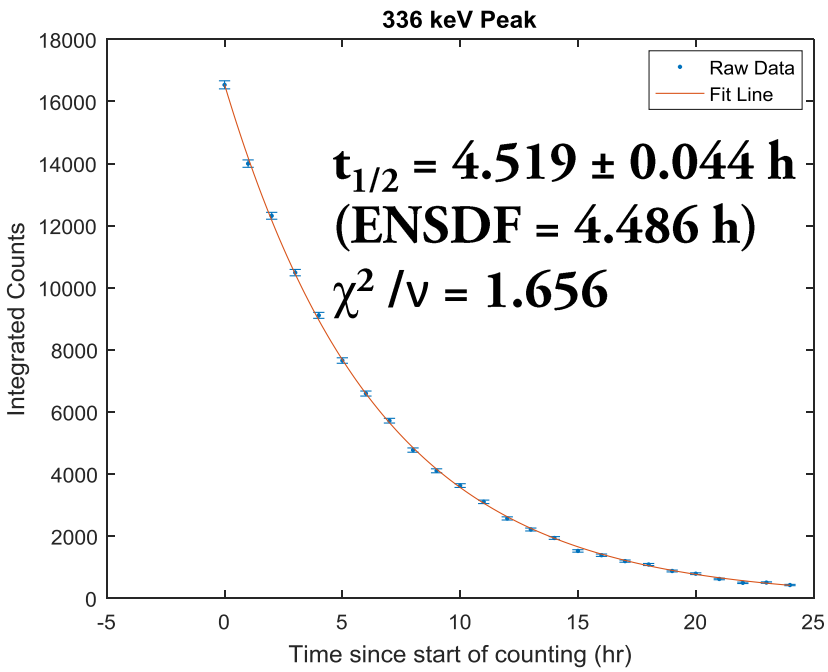

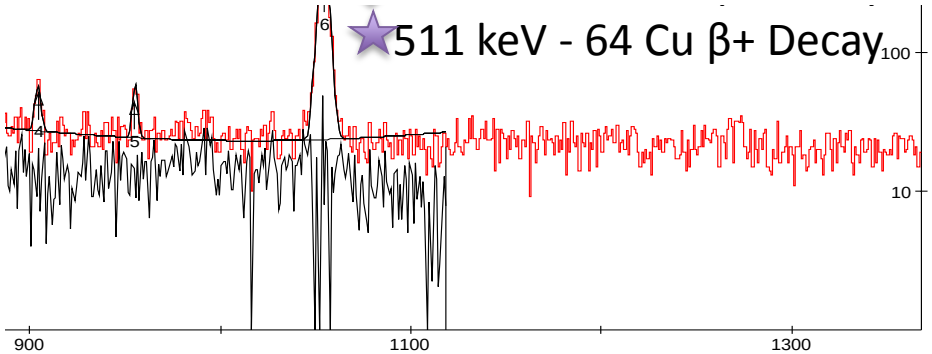

Relative Activation Measurements

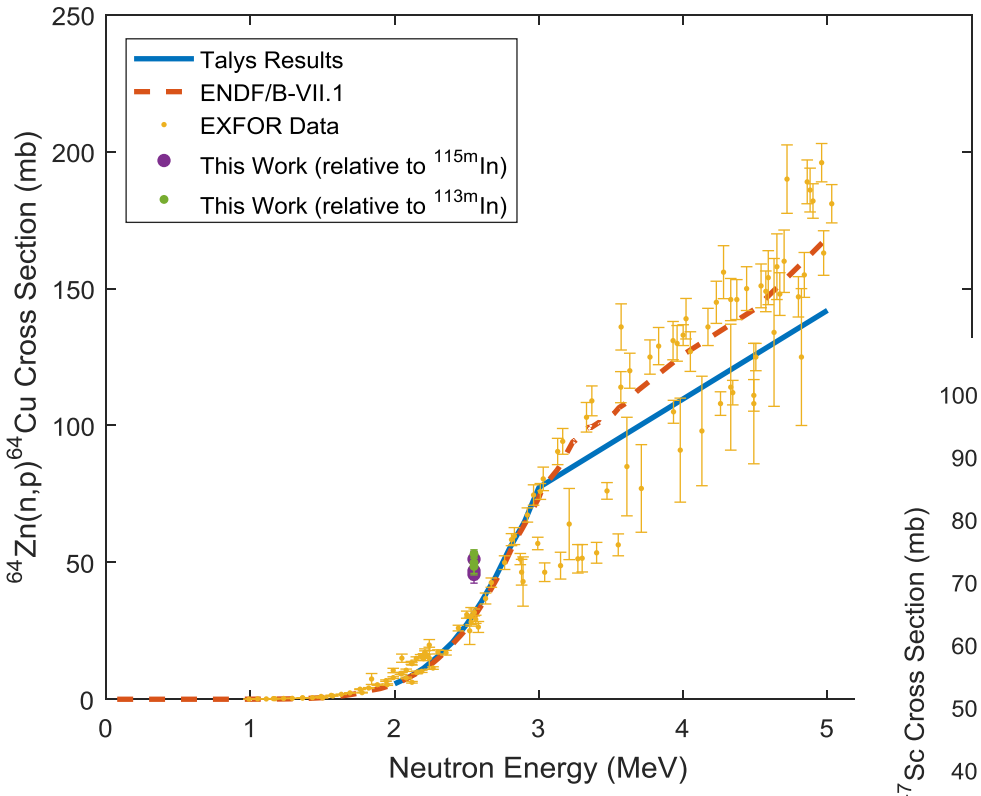

What's going on???

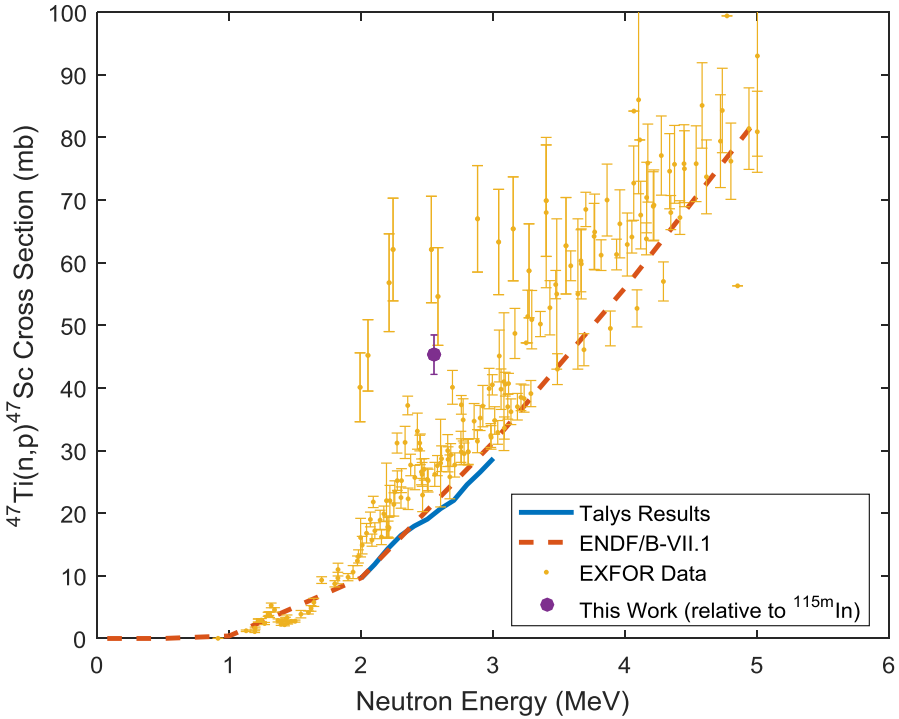

Neutron Energy Spread

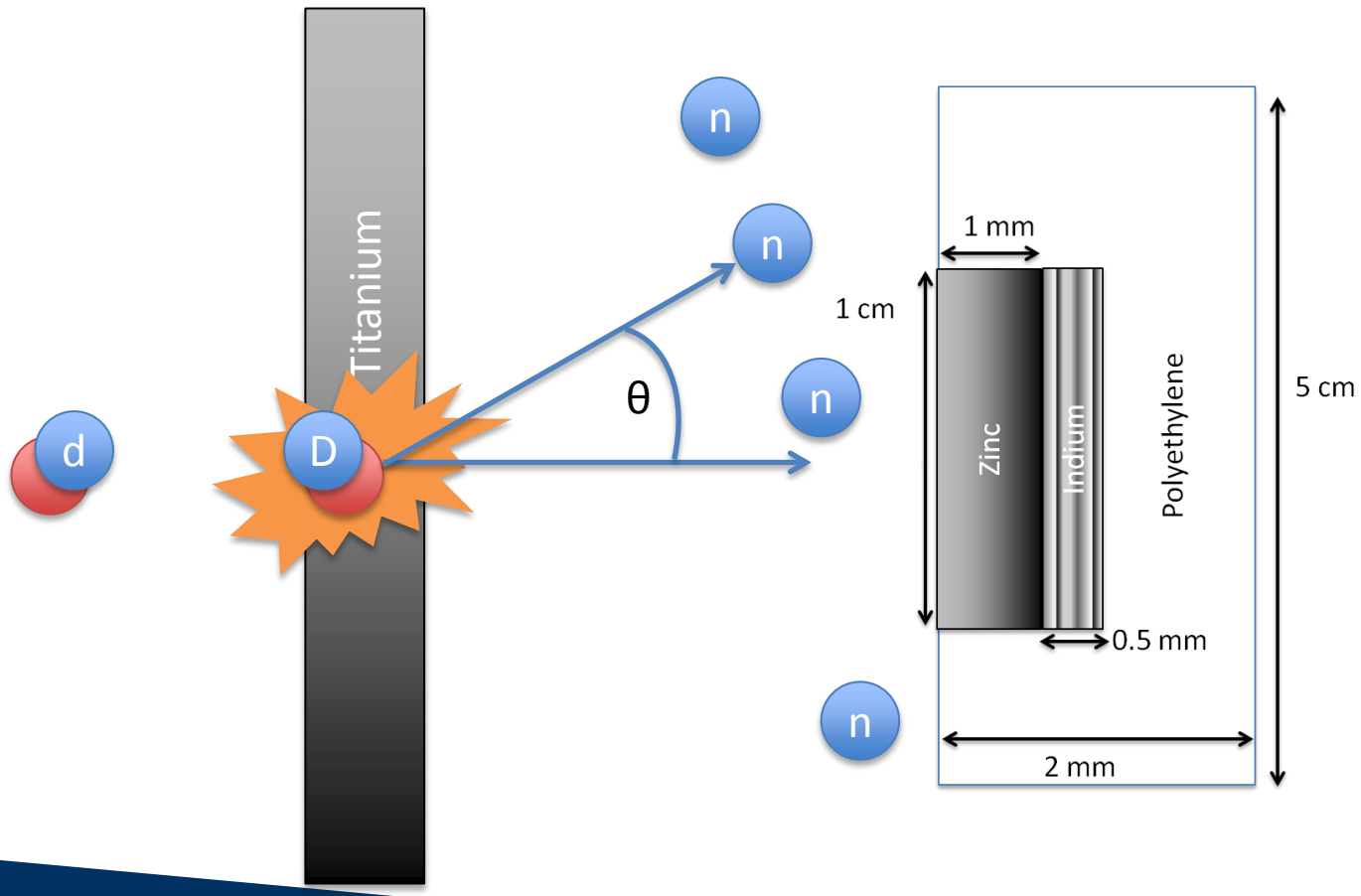

Neutron Energy Spread

H. Liskien *et al.*, Nucl Data Tables, vol 11, 2973

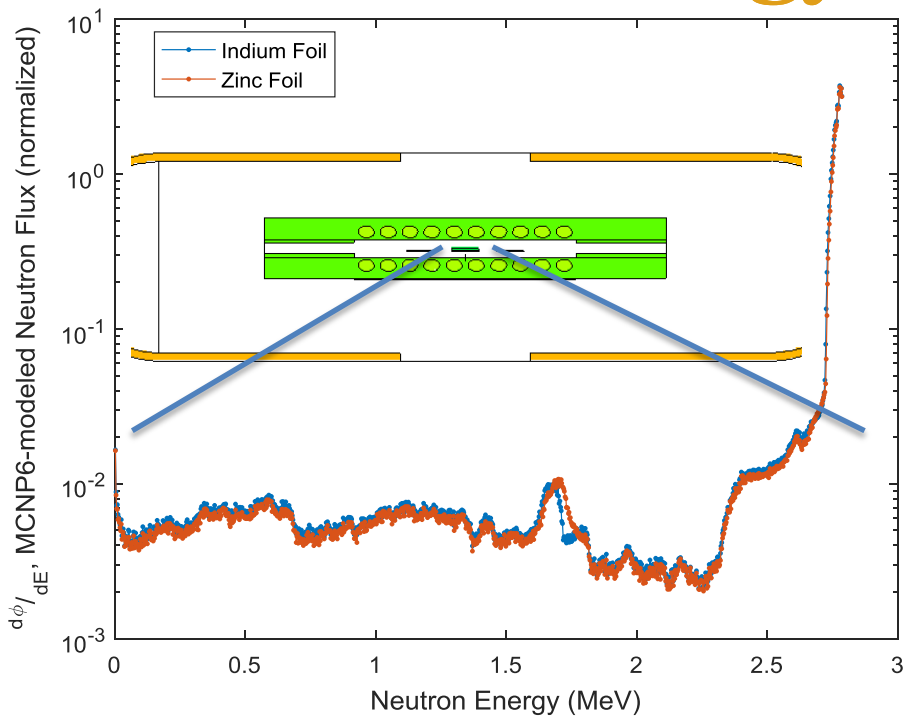

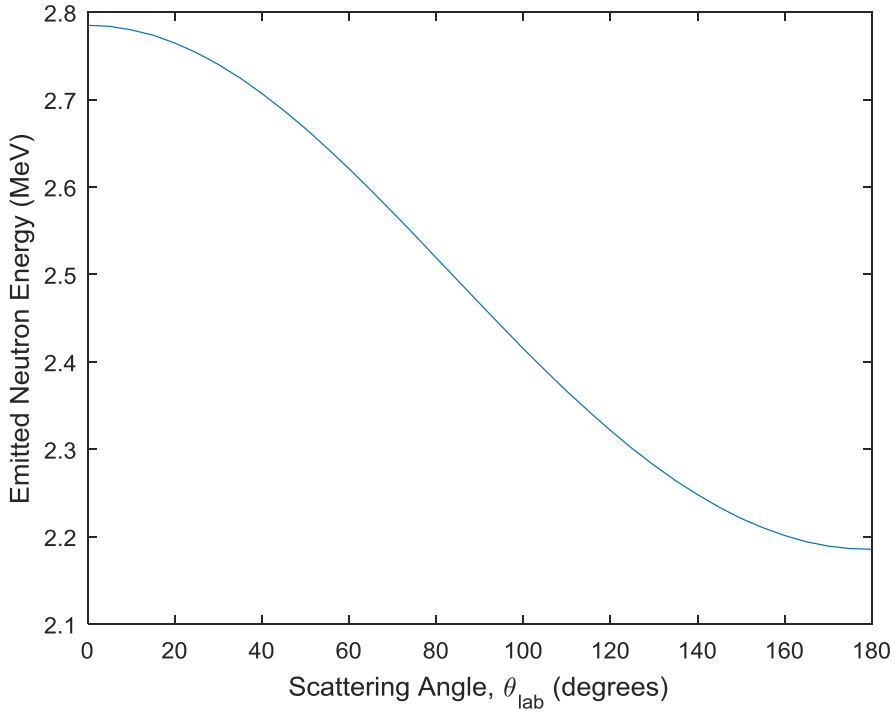

Neutron flux profile modeled in target and monitor foil, using MCNP6

Neutron Energy Spread

H. Liskien *et al.*, Nucl Data Tables, vol 11, 2973

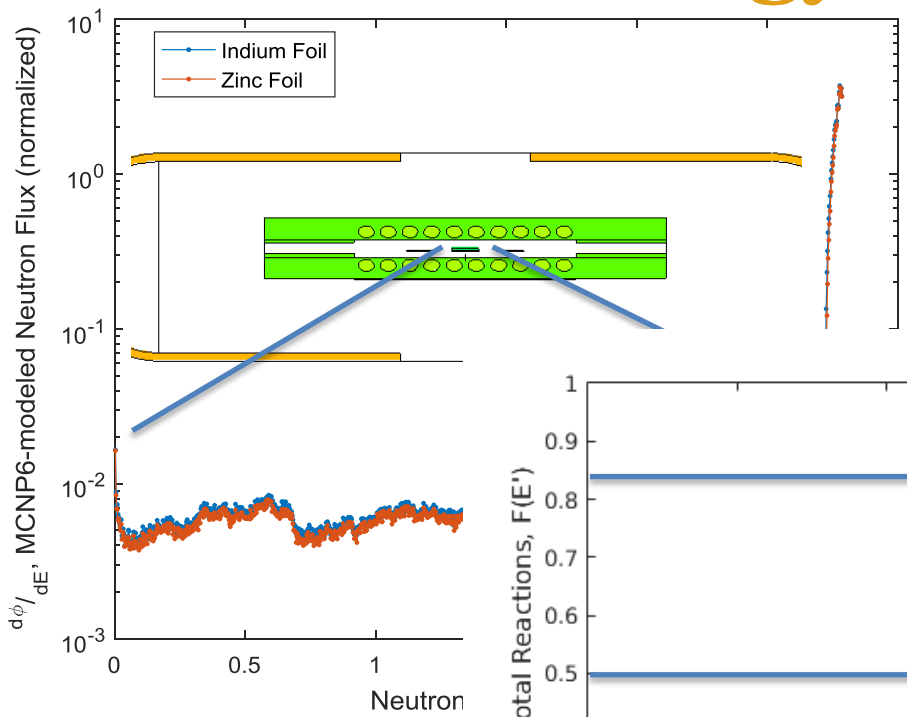

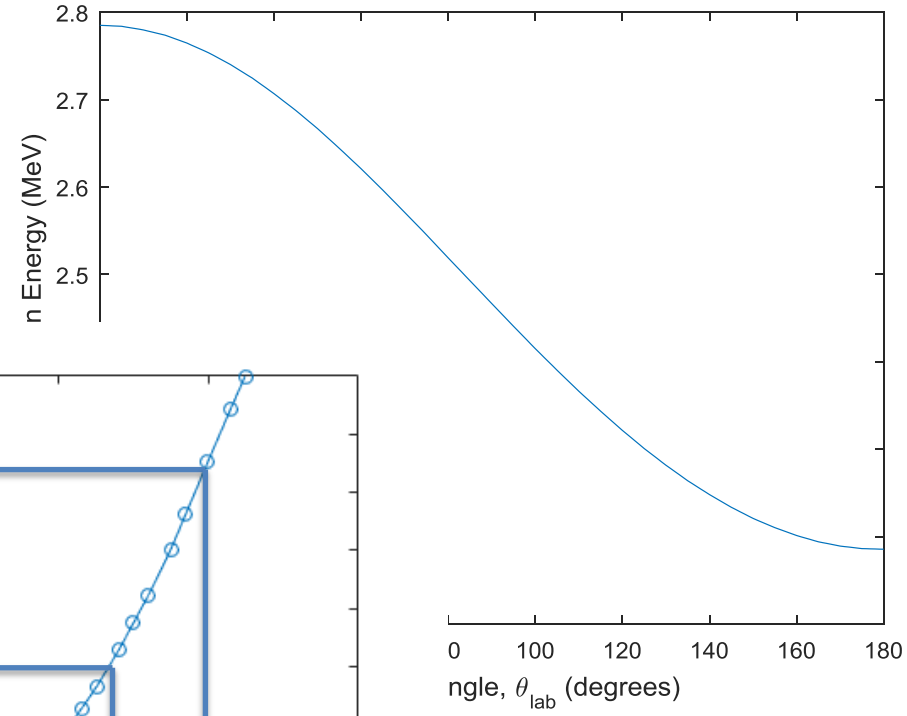

Neutron flux in target and using MCNP6

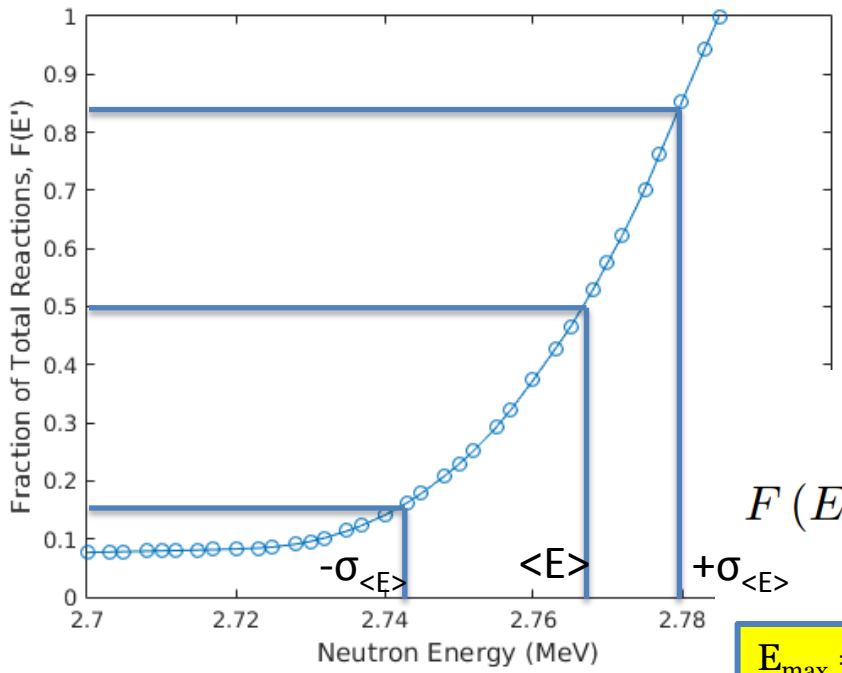

$$F(E') = \frac{\int_0^{E'} \sigma(E) \frac{d\phi}{dE} dE}{\int_0^{E_{max}} \sigma(E) \frac{d\phi}{dE} dE}$$

E_{max} = Maximum energy neutron subtended by foil
F(E') = Fraction of Total Reactions induced up to energy E'

Neutron Energy Spread

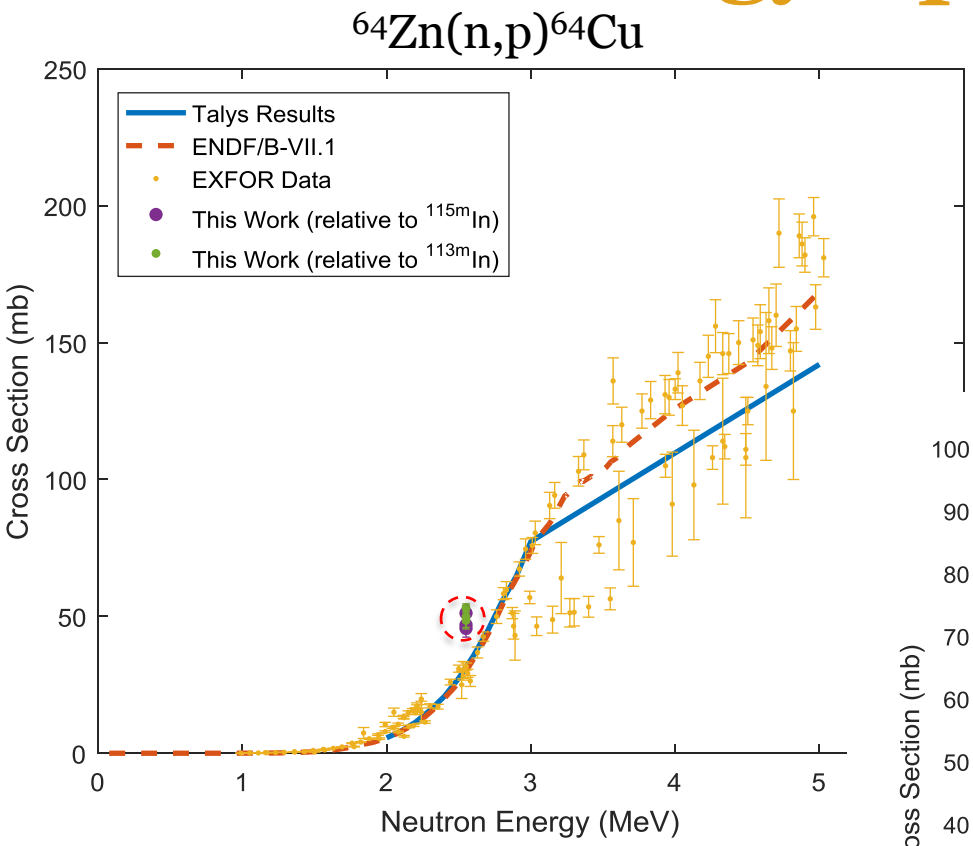

Before…

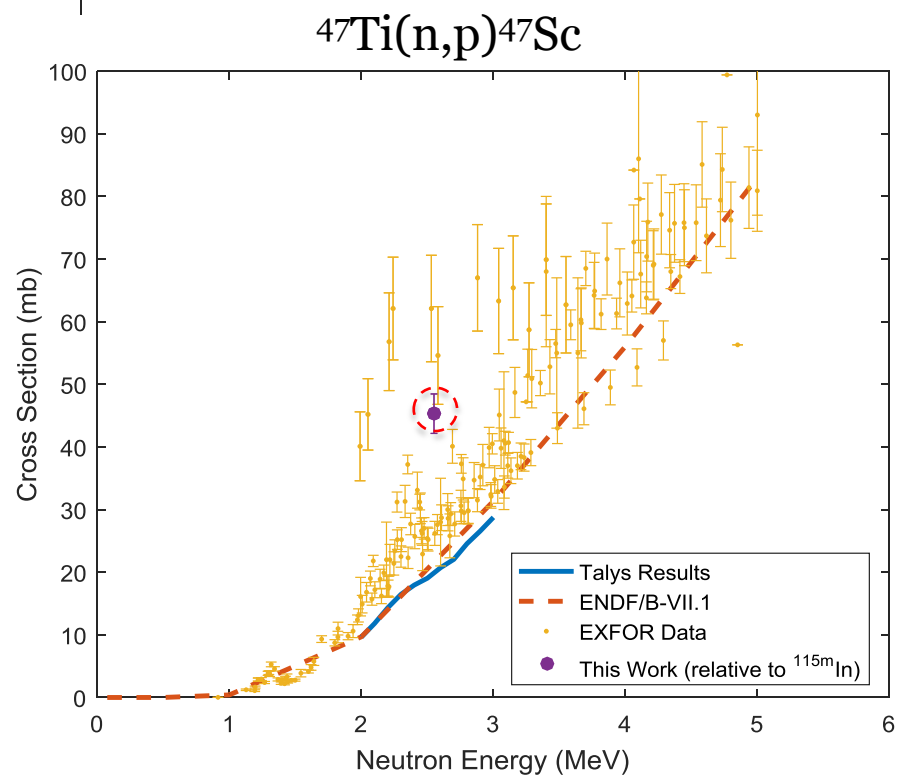

Neutron Energy Spread

Table 3. Results of cross section measurement.

Reaction	$\sigma(E_n = 2.7645$ MeV) (mb)
^{64}Zn(n,p)^{64}Cu (relative to ^{113}In)	45.953 ± 3.351, 46.493 ± 2.805, 46.9 ± 3.189
^{64}Zn(n,p)^{64}Cu (relative to ^{115}In)	49.716 ± 3.335, 49.011 ± 2.698,
^{47}Ti(n,p)^{47}Sc (relative to ^{115}In)	25.901 ± 1.7089,

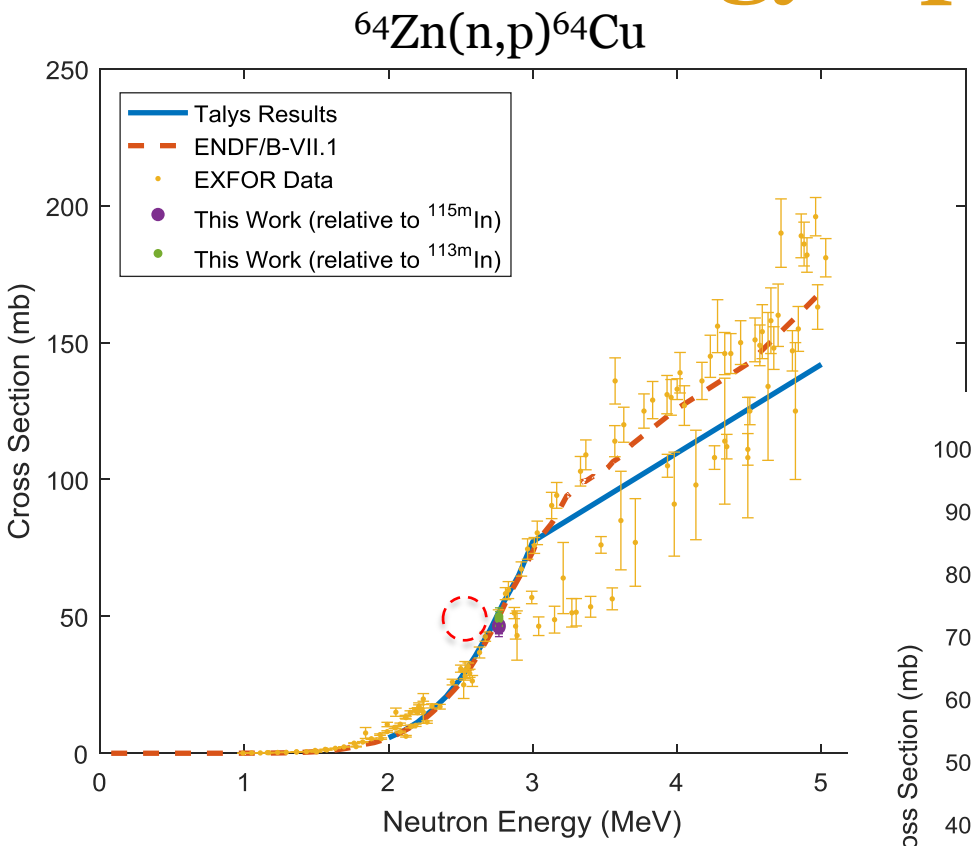

After!

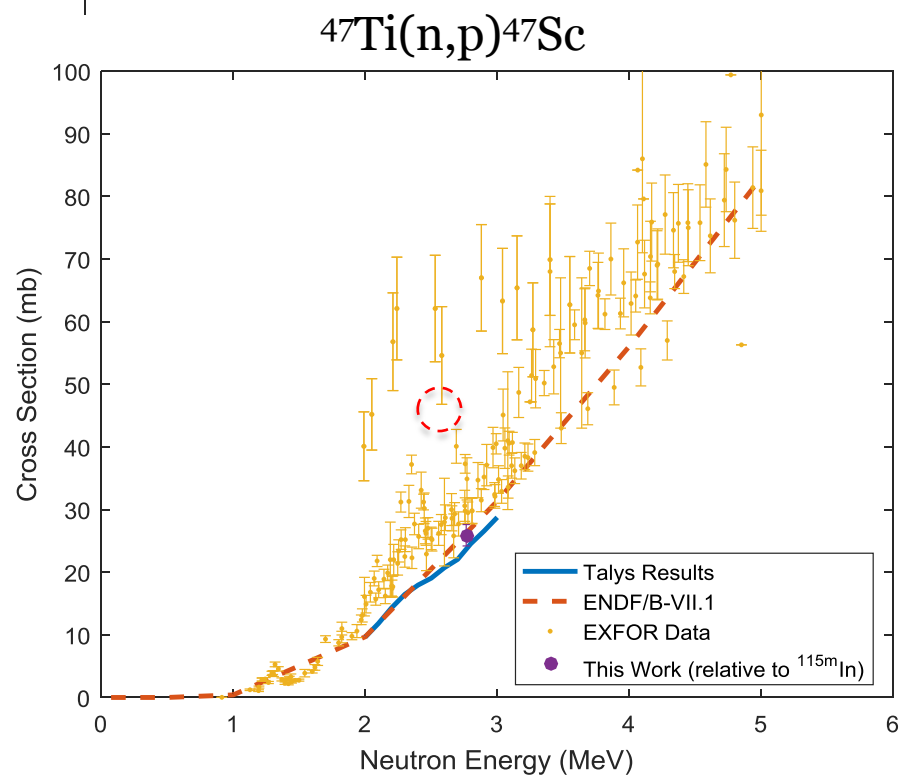

Neutron Energy Spread

Table 3. Results of cross section measurement.

Reaction	$\sigma(E_n = 2.7645$ MeV) (mb)
^{64}Zn(n,p)^{64}Cu (relative to ^{113}In)	45.953 ± 3.351, 46.493 ± 2.805, 46.9 ± 3.189
^{64}Zn(n,p)^{64}Cu (relative to ^{115}In)	49.716 ± 3.335, 49.011 ± 2.698,
^{47}Ti(n,p)^{47}Sc (relative to ^{115}In)	25.901 ± 1.7089,

^{64}Zn(n,p)^{64}Cu

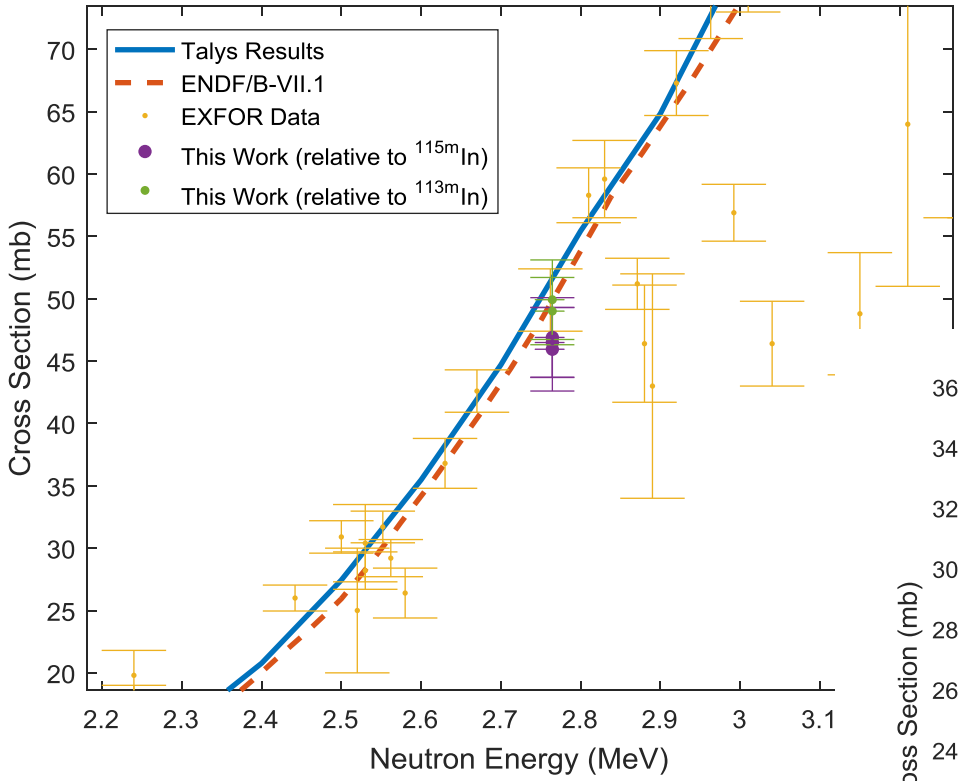

After!

^{47}Ti(n,p)^{47}Sc

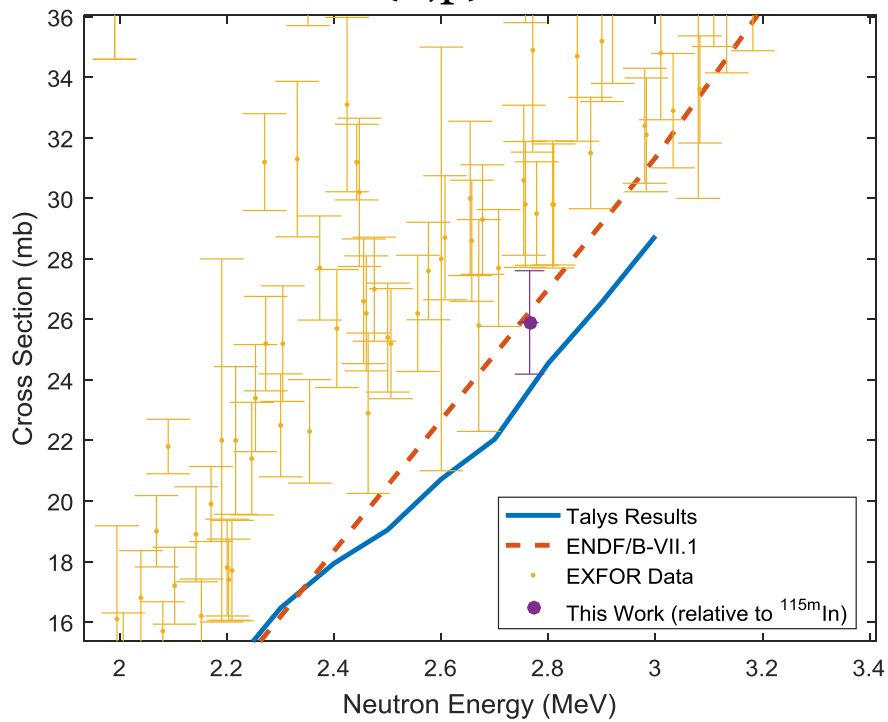

Future Work

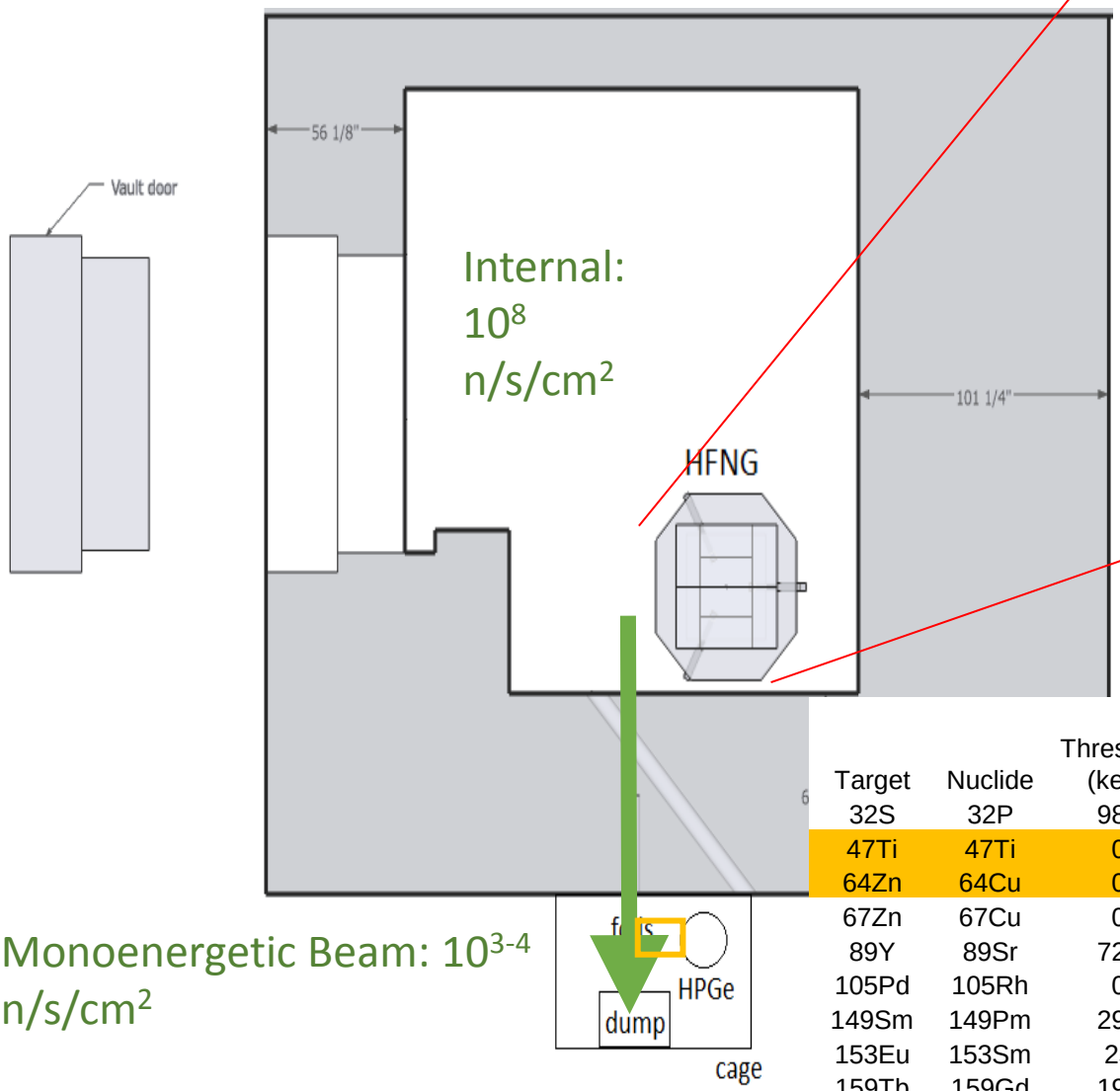

Phase 1 current upgrade complete!

Monoenergetic Beam: $10^{3\text{-}4}$ n/s/cm^2

Target	Nuclide	Threshold (keV)	% abundance	Strongest γ-ray branch (keV)	# seen in a 0.5% Ge detector	Rate in a 0.5% detector
32S	32P	985	95%	0	0.00E+00	0.00
47Ti	47Ti	0	7.44%	159.381	1.24E+05	1.44
64Zn	64Cu	0	49.20%	511	5.03E+05	5.82
67Zn	67Cu	0	4.04%	184.577	5.45E+04	0.63
89Y	89Sr	726	100%	908.96	1.25E+02	0.00
105Pd	105Rh	0	22.33%	318.9	1.27E+05	1.47
149Sm	149Pm	291	11.24%	285.94	4.47E+03	0.05
153Eu	153Sm	25	52.19%	103.18	1.36E+05	1.58
159Tb	159Gd	190	100%	363.543	1.58E+05	1.83
161Dy	161Tb	0	18.89%	75.57	2.66E+04	0.31
166Er	166Ho	1079	33.50%	1379.4	4.39E+03	0.05
169Tm	169Er	0	100%	109.8	1.87E+01	0.00
175Lu	175Yb	0	97.40%	396.3	1.88E+05	2.18
177Hf	177Lu	0	18.60%	208.4	3.77E+04	0.44

Stacked-target Charged Particle Excitation Functions

LBNL

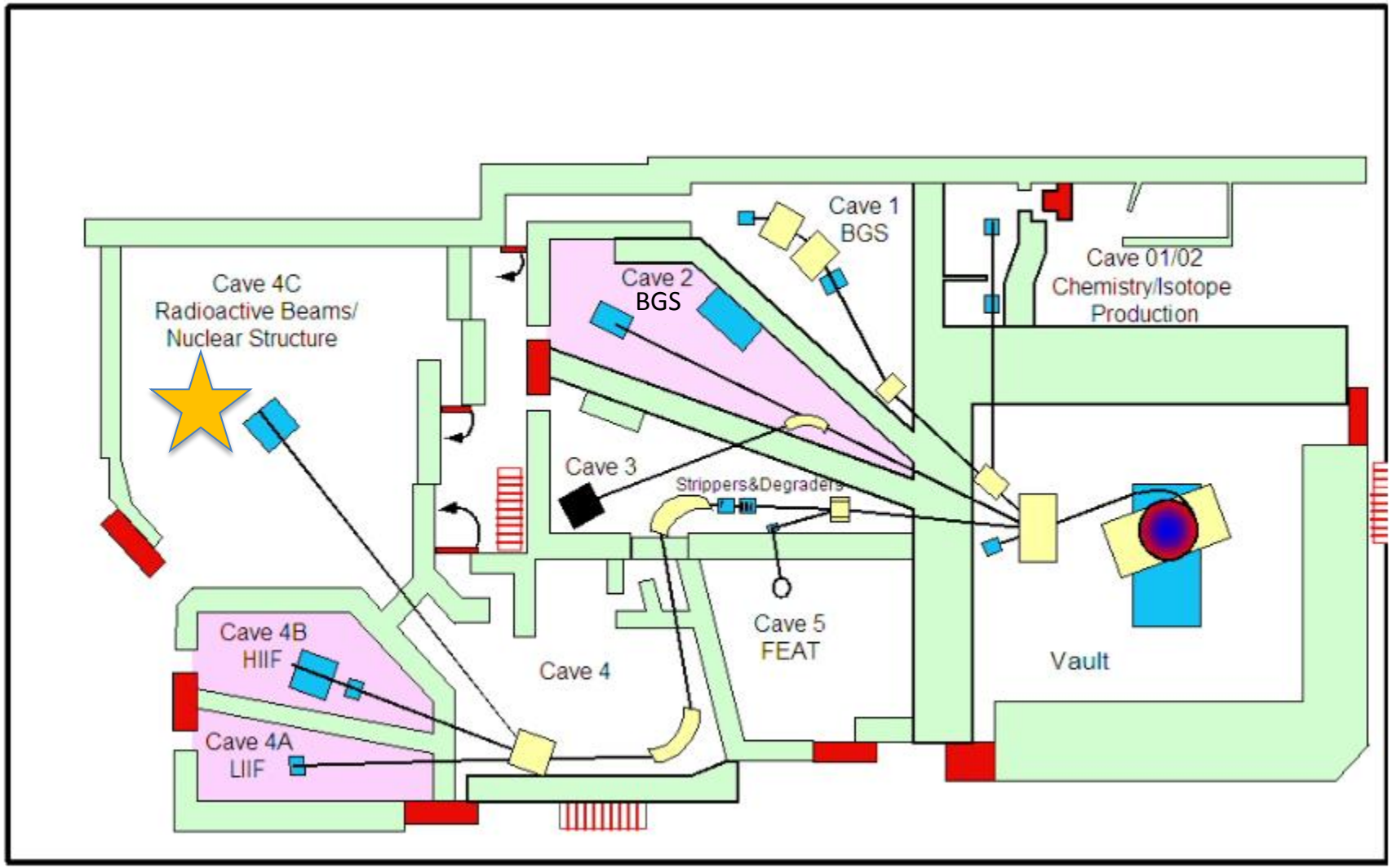
Cave 1
BGS
Cave 01/02
Chemistry/Isotope
Production
Cave 4C
Radioactive Beams/
Nuclear Structure
Cave 2
BGS
Cave 3
Strippers&Degraders
Cave 5
FEAT
Cave 4B
HIIF
Cave 4
Vault
Cave 4A
LIIF

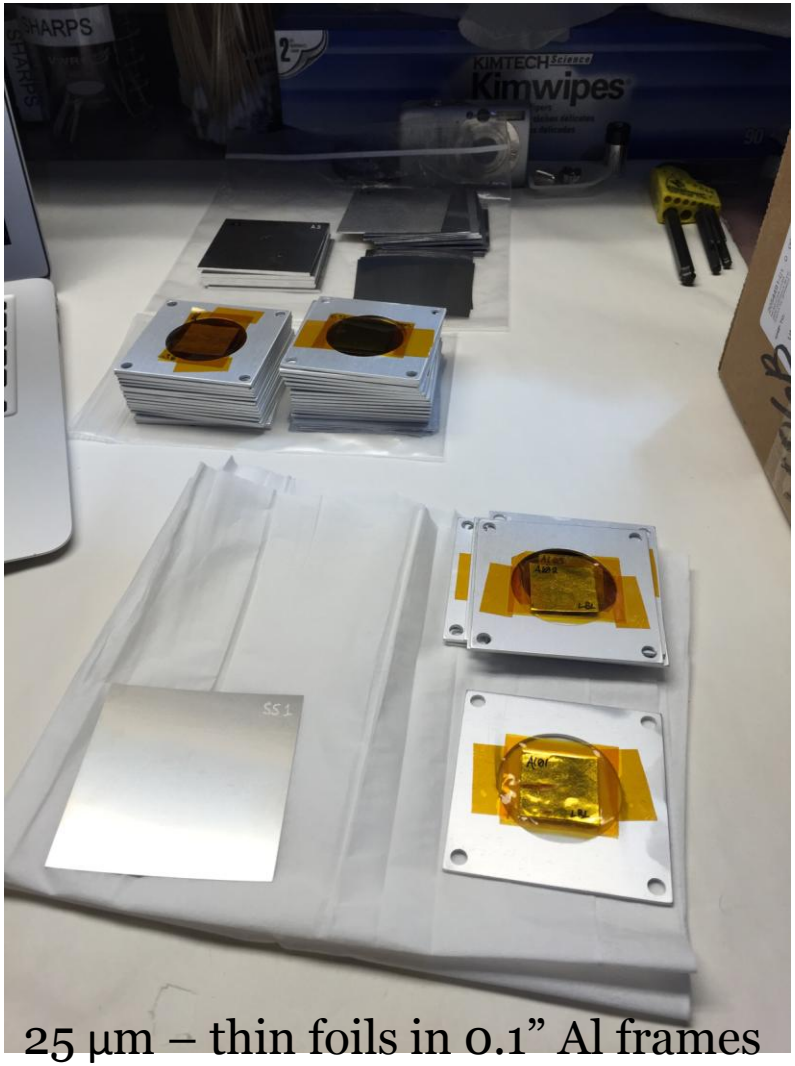

25 µm – thin foils in 0.1” Al frames

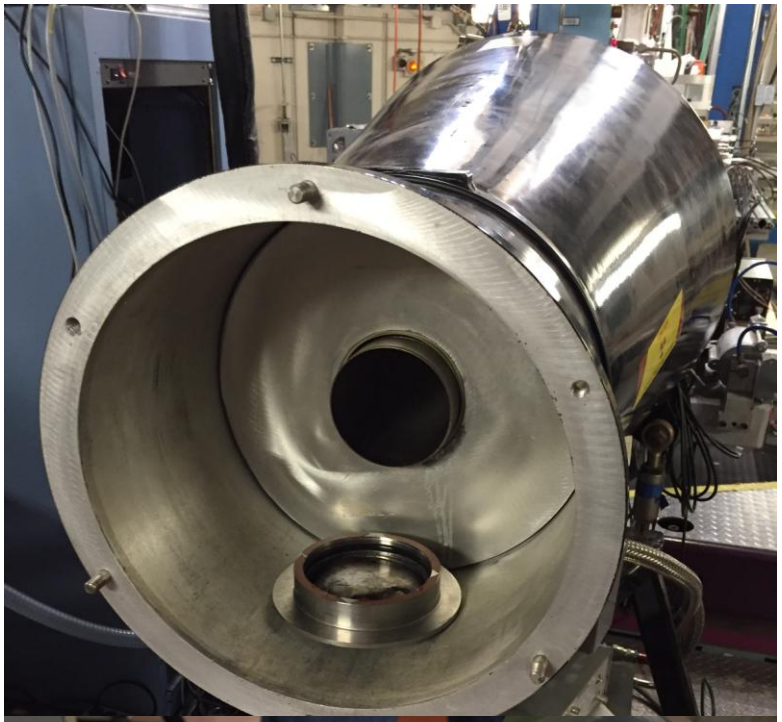

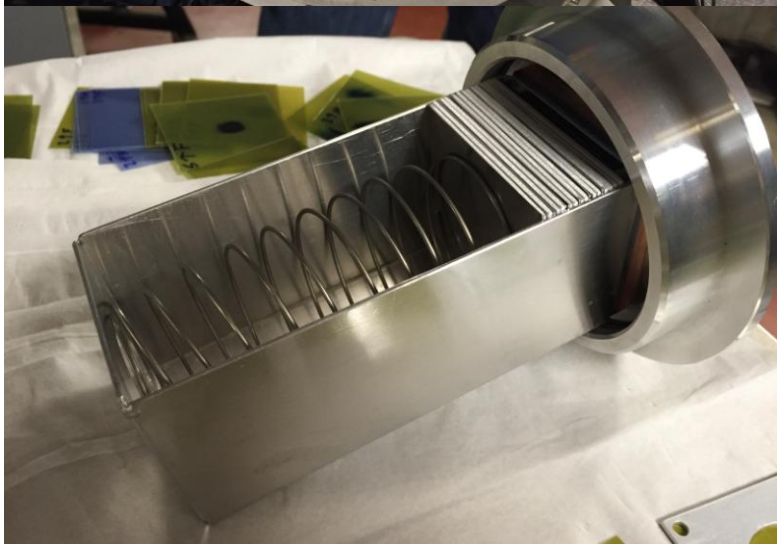

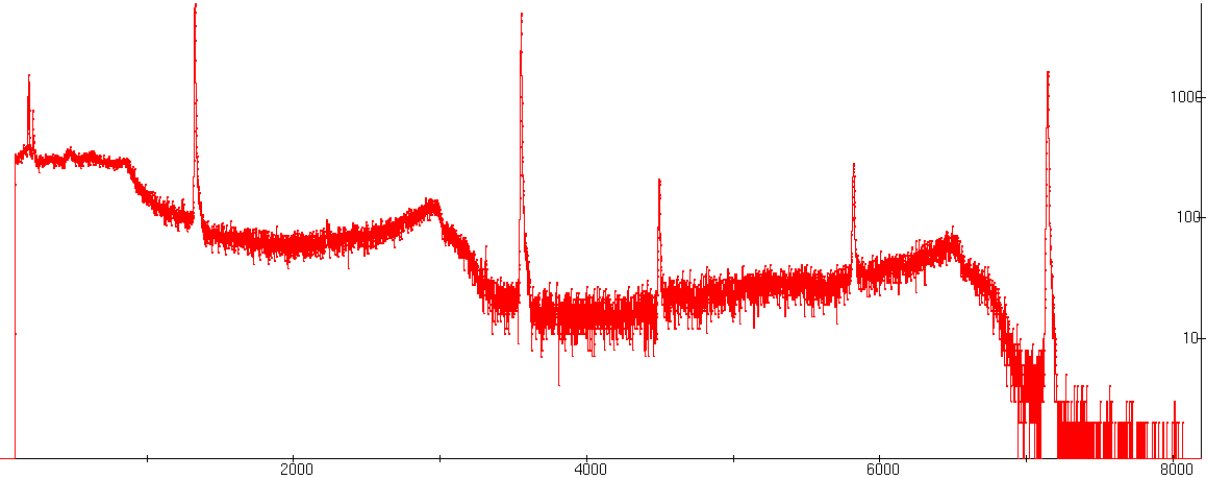

Al Spectra

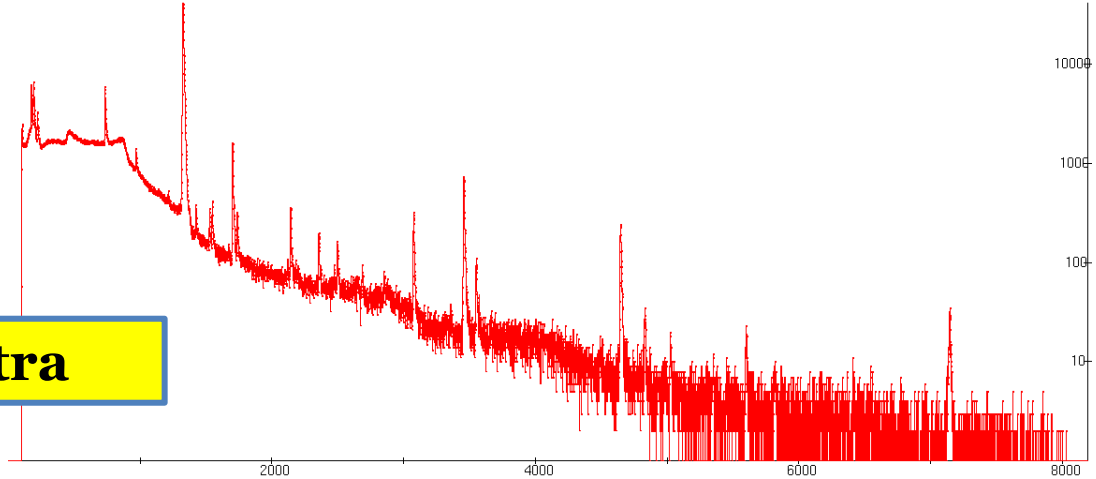

Cu Spectra

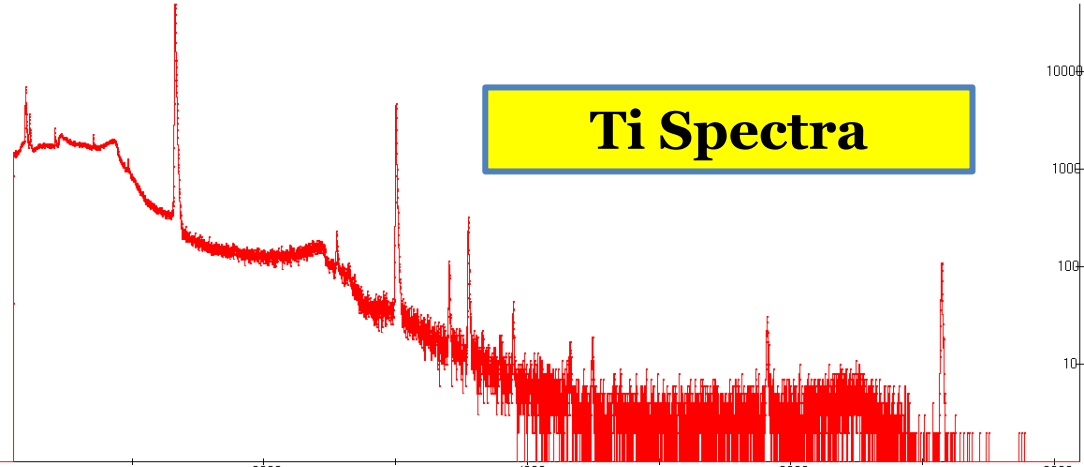

Ti Spectra

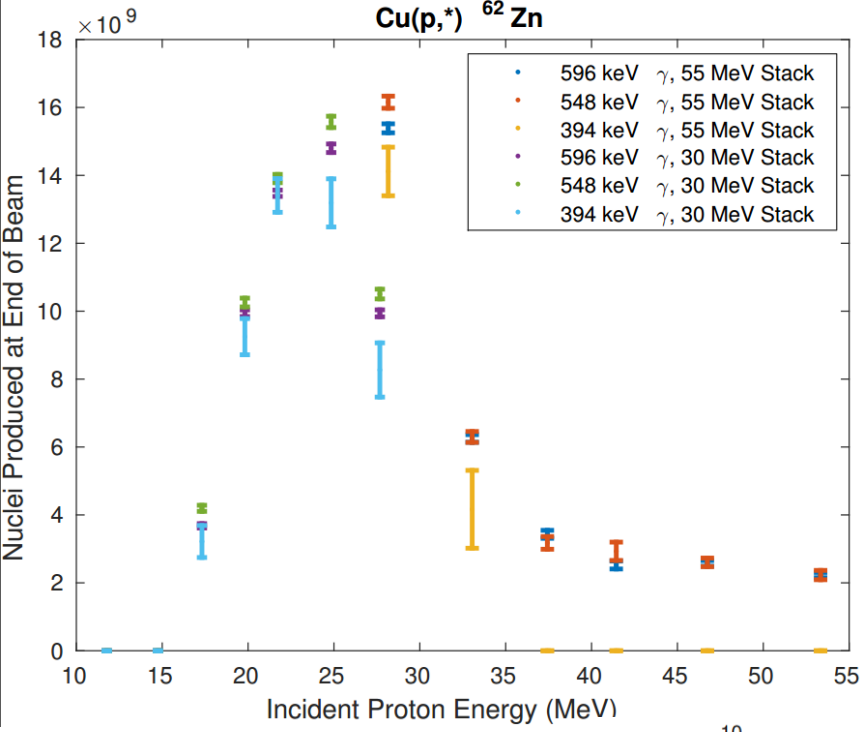

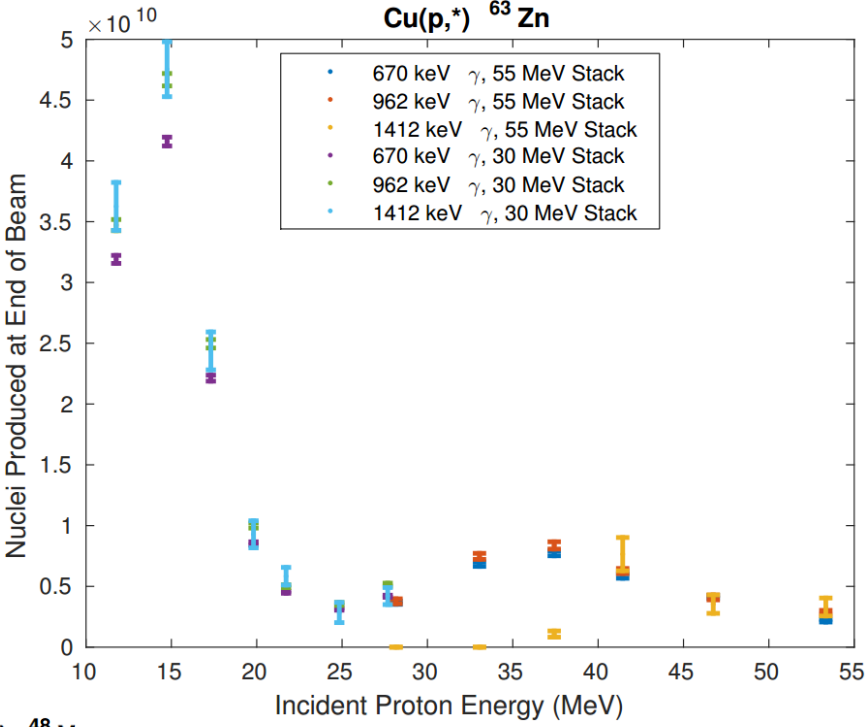

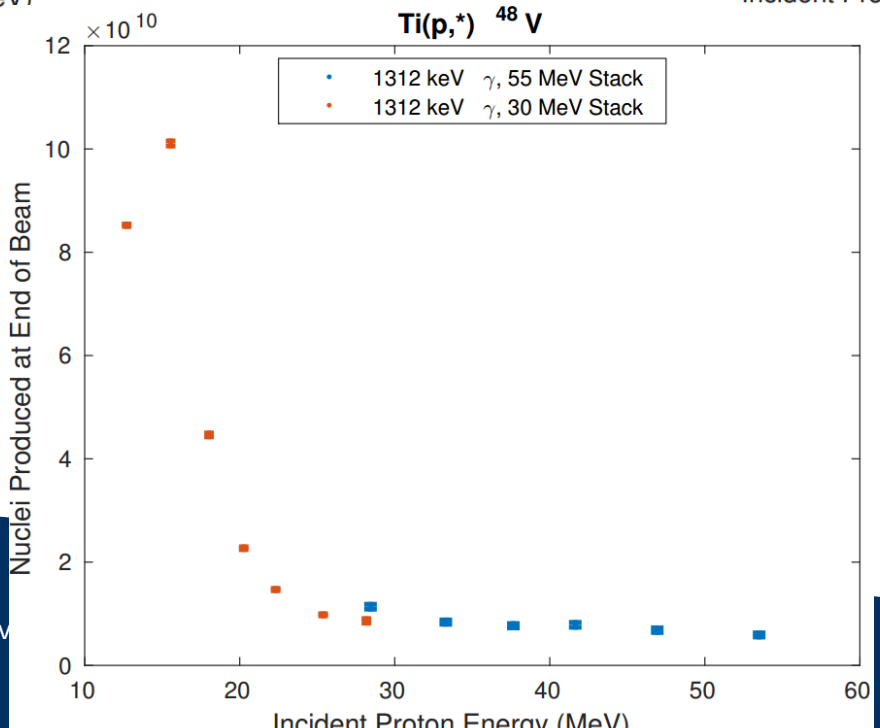

Preliminary results

Berkeley
UNIVERSITY OF CALIFORNIA

Tunable Neutron Source

LBNL

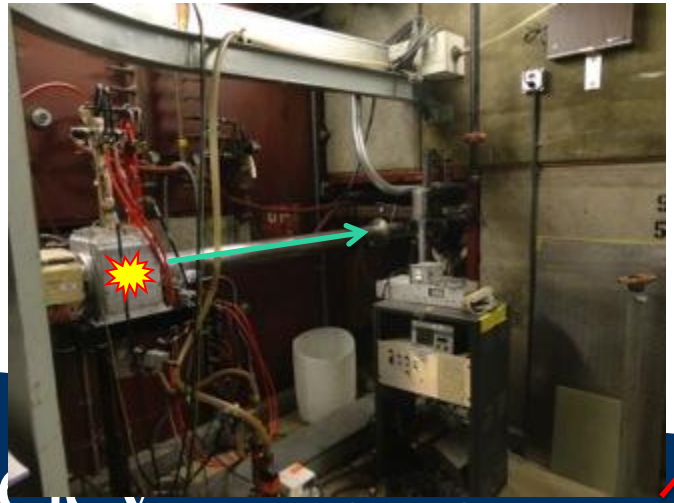

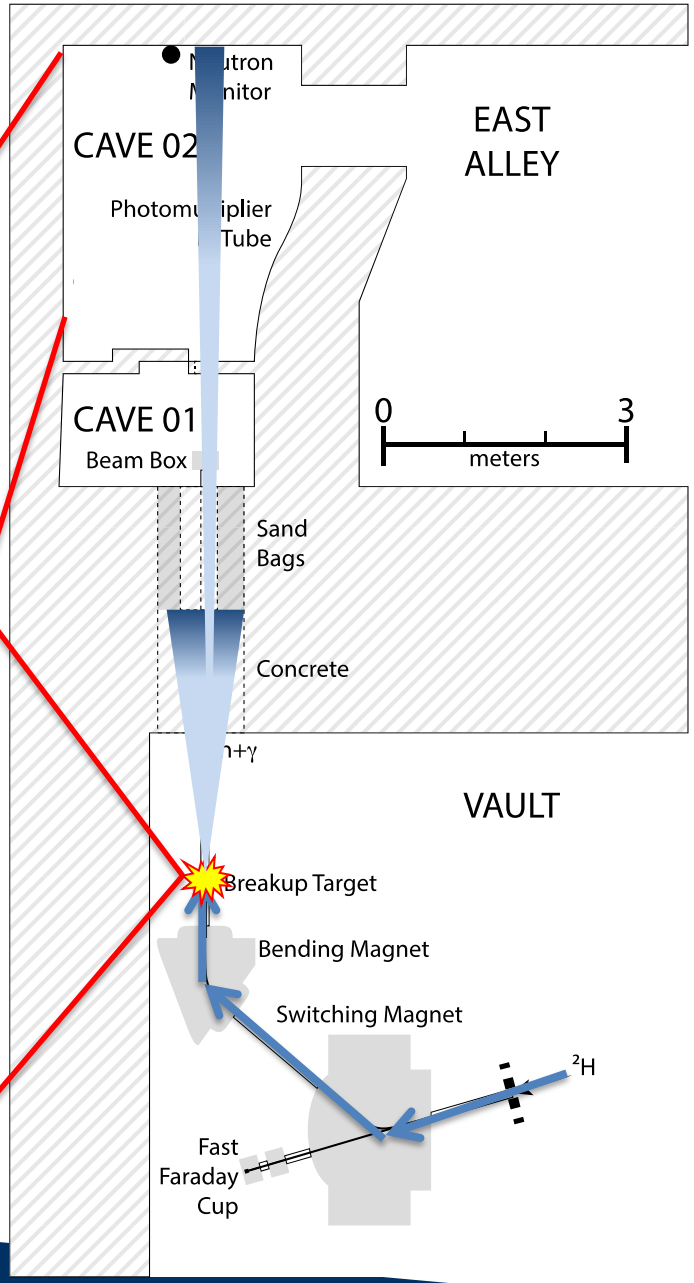
CAVE 02
EAST
ALLEY
CAVE 01
Beam Box
0
3
meters
Sand
Bags
Concrete
VAULT
Breakup Target
Bending Magnet
Switching Magnet
^{2}H
Fast
Faraday
Cup

10-cm-radius, well-collimated, open-air neutron beam

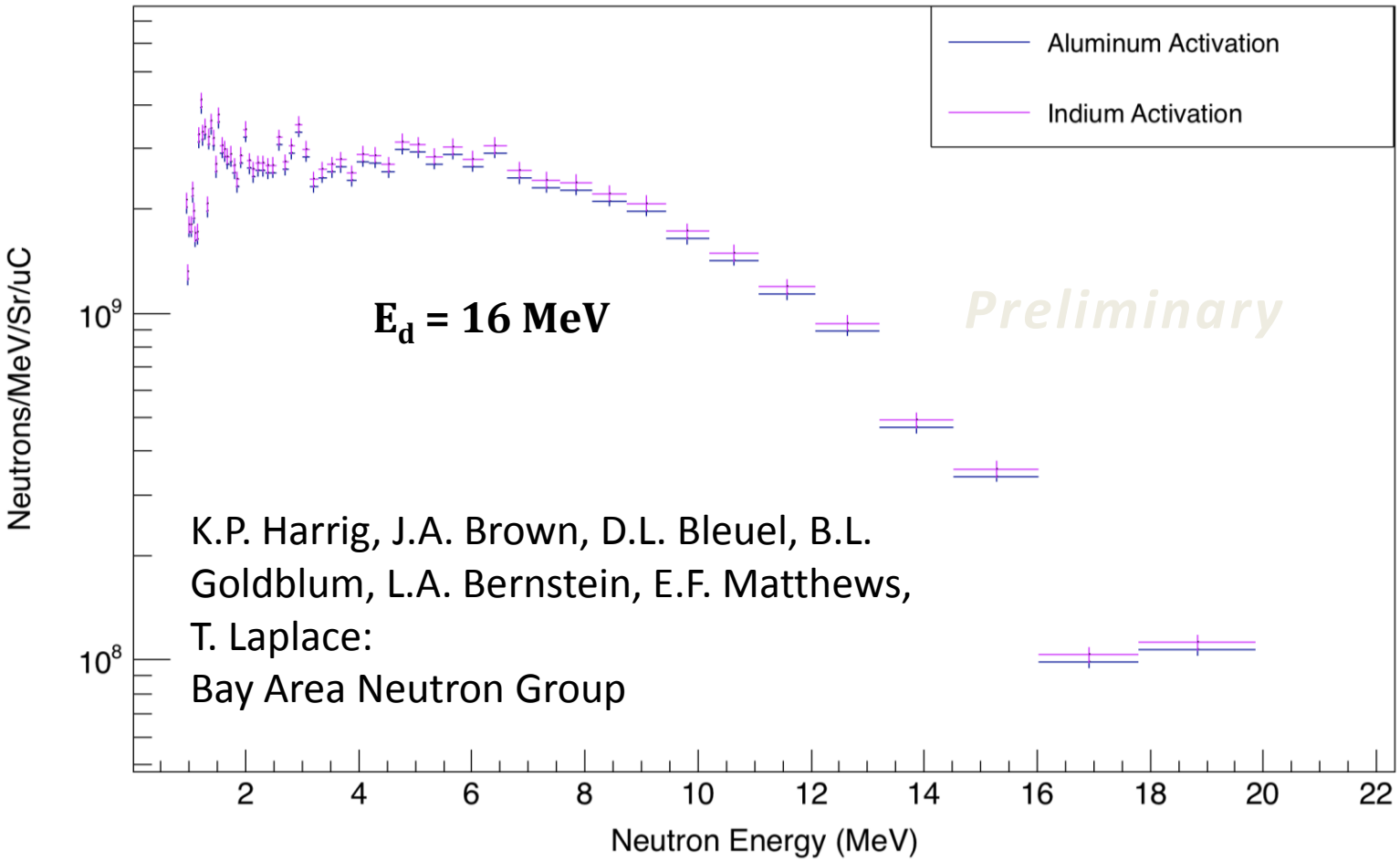

K.P. Harrig, J.A. Brown, D.L. Bleuel, B.L. Goldblum, L.A. Bernstein, E.F. Matthews, T. Laplace:
Bay Area Neutron Group

^{56}Fe Structure

GRETINA @ ANL

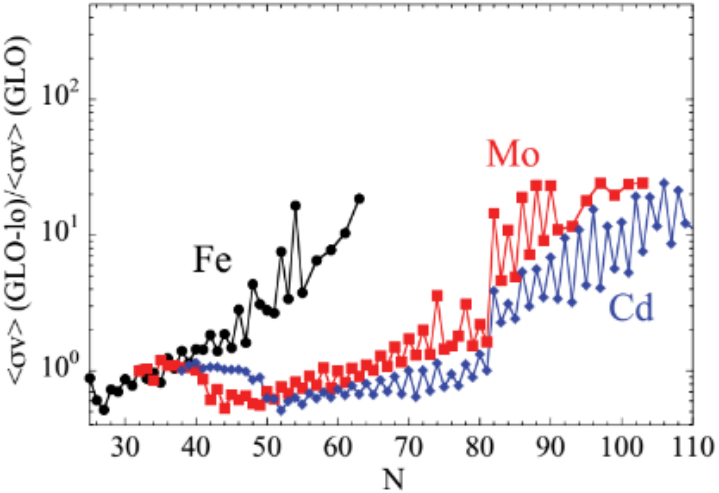

FIG. 5. (Color online) Ratios of Maxwellian-averaged (n,γ) reaction rates at $T = 10^9$ K for the Fe, Mo, and Cd isotopic chains up to the neutron drip line, using the GLO-lo and GLO model.

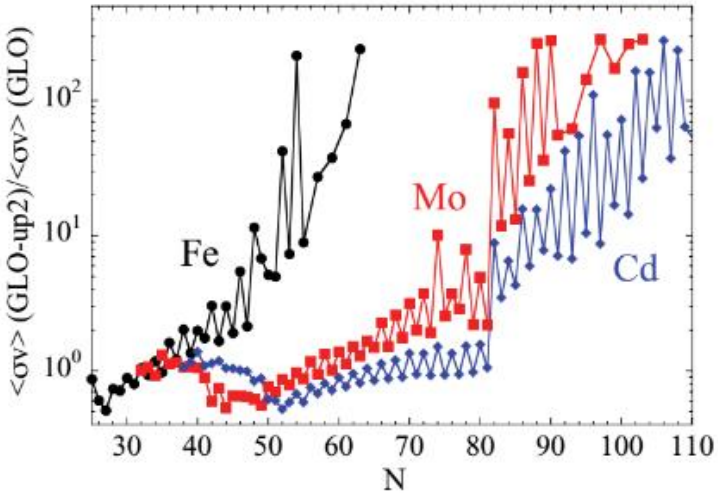

FIG. 7. (Color online) Same as Fig. 5 for the GLO-up2 and the GLO model.

Larsen *et al*, DOI: 10.1103/PhysRevC.82.014318

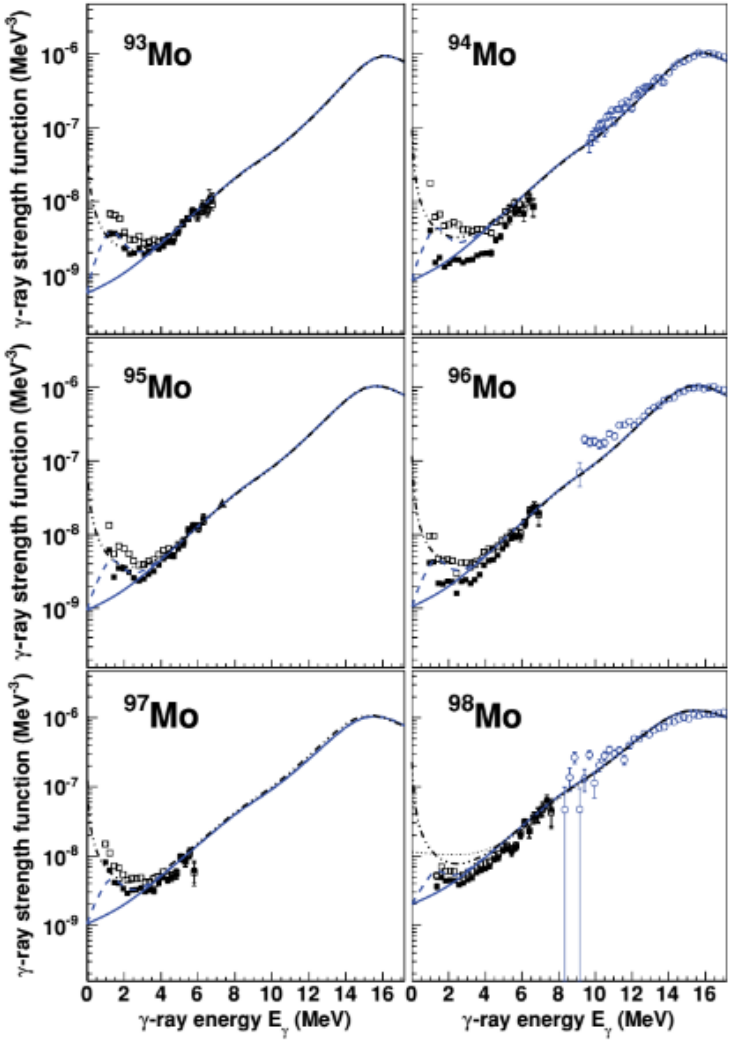

FIG. 3. (Color online) Gamma-ray strength functions for $^{93-98}$Mo. Experimental data points with the normalization of Ref. [6] are shown as open squares. The filled squares are obtained when normalizing the experimental NLDs on the basis of the calculations of [20]. Giant resonance photoabsorption data (blue open circles) for ^{94,96,98}Mo are taken from [32]. The black triangles represent measured $E1$ strengths for ^{93,95}Mo from [15]. The blue solid line corresponds to the GLO-lo parametrization, the blue dashed line to the GLO-up1 parametrization, and the dash-dot line shows the GLO-up2 model. For ^{98}Mo, also the GLO model for $E_n = 1$ MeV is displayed (dotted line).

Leo Kirsch
UC Berkeley
4th year PhD student

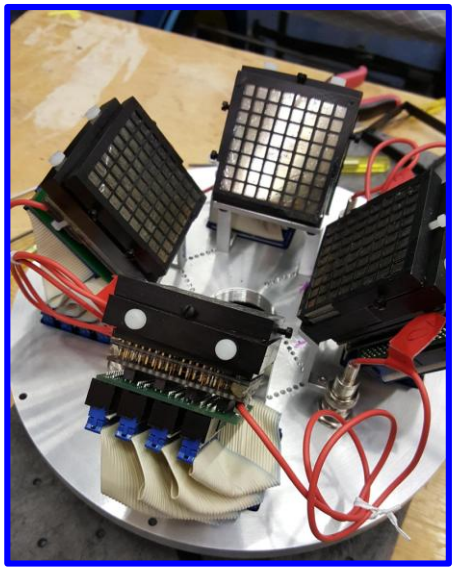

LBNL GRETINA Team
$^{56}Fe(p,p'\gamma)$ @ Argonne

Level Scheme
Low lying lifetimes

Phoswich Wall:
E_p, θ_p

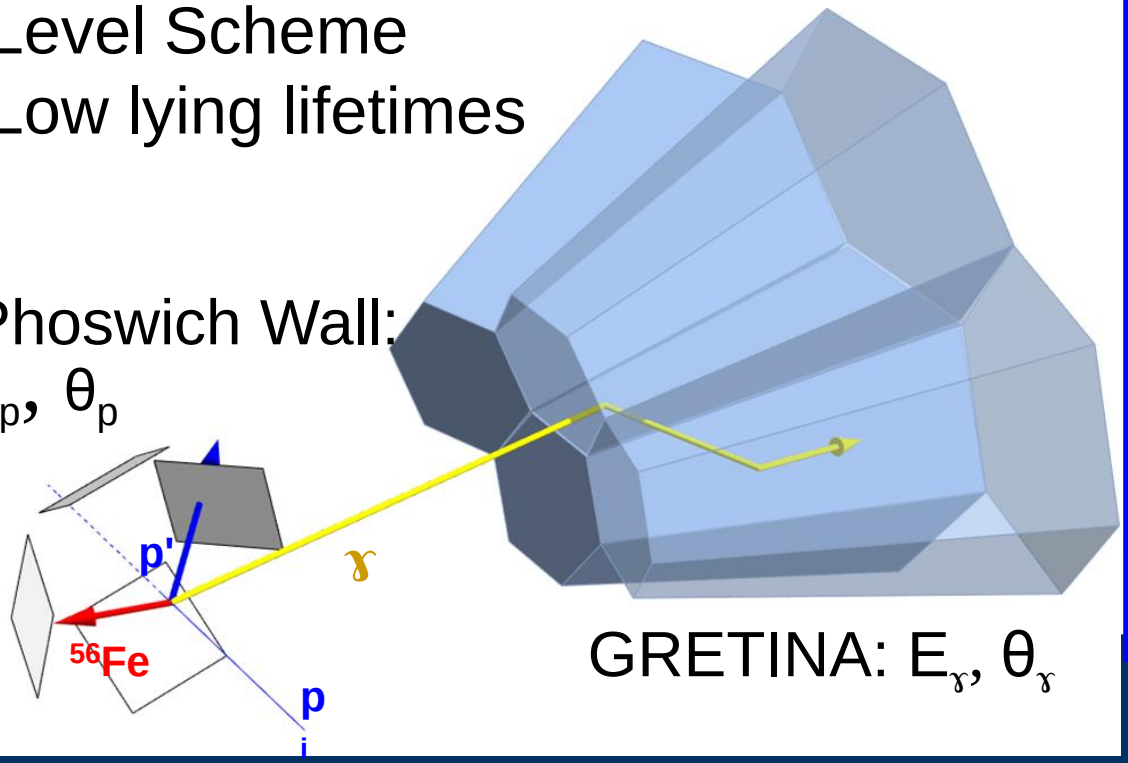

GRETINA: E_γ, θ_γ

$^{56}Fe(p,p'\gamma)$ Level Scheme (partial)

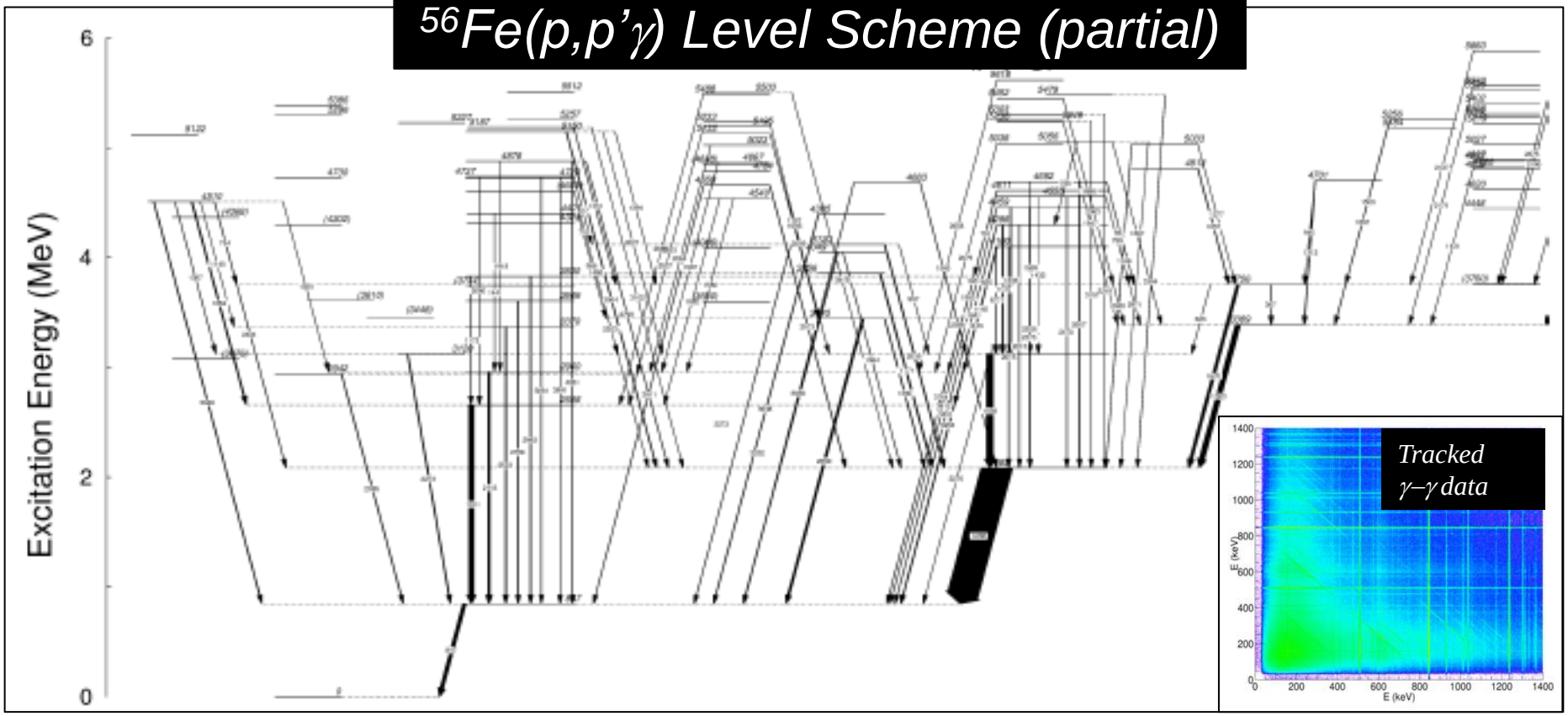

Doppler Shift

$^{56}Fe\ 2^+_2 \rightarrow 2^+_1$

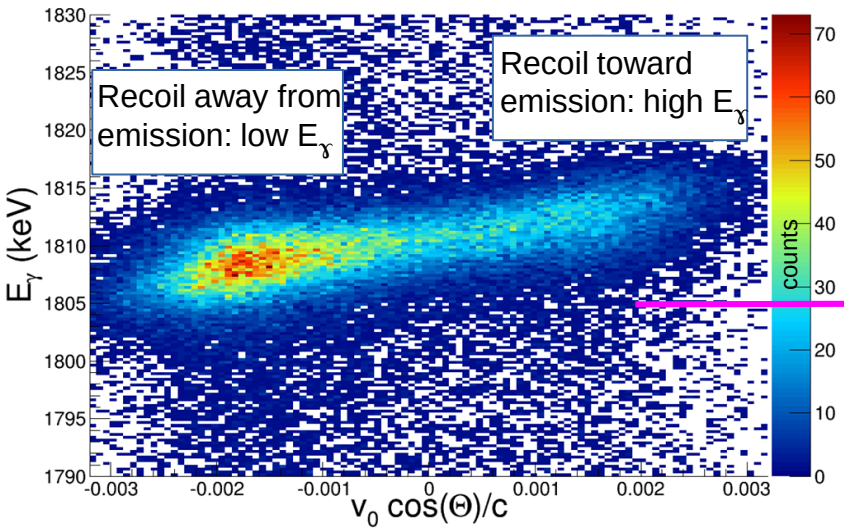

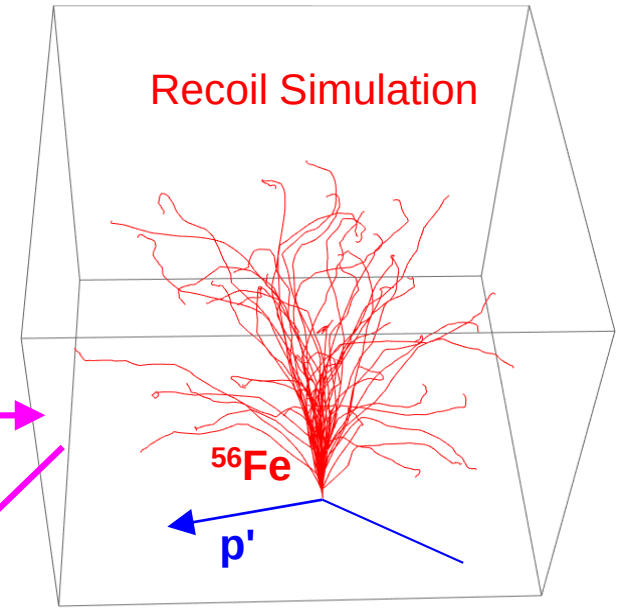

After $t_{1/2}$=30 fs correction

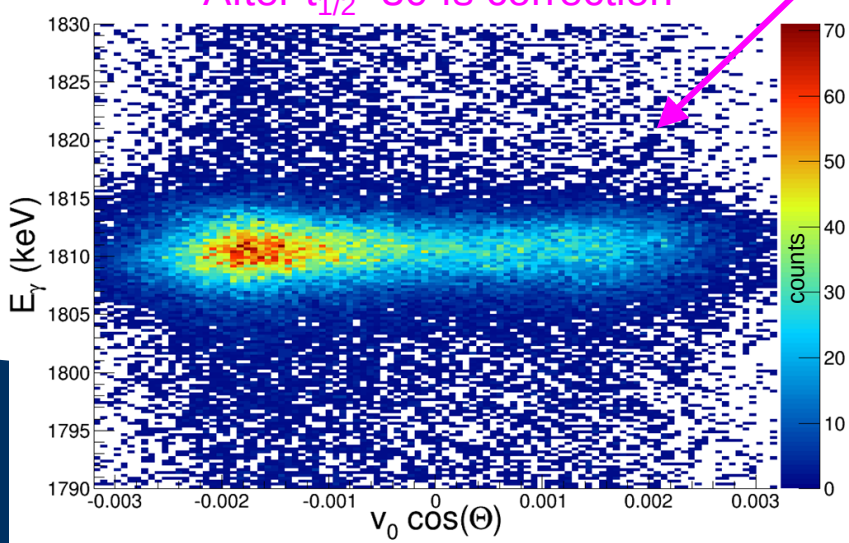

Lvl(keV)	E_γ(keV)	Transition	This Work $t_{1/2}$ (fs)	ENSDF Comparison (n,n')	ENSDF Comparison (p,p')
2657	1810	$2^+_2 \rightarrow 2^+_1$	**33(2)**	21(1)	28(7)
2960	2113	$2^+_3 \rightarrow 2^+_1$	**20(4)**	28(3)	27(9)
3120	2273	$1^+_1 \rightarrow 2^+_1$	**20(8)**	19(1)	24(11)
3123	1037	$4^+_2 \rightarrow 4^+_1$	**51(4)**	47(12)	50^{+50}_{-30}
3370	2523	$2^+_4 \rightarrow 2^+_1$	**19(2)**	17(3)	18(7)
3445	2598	$3^+_1 \rightarrow 2^+_1$	**<52**	29(5)	<28

Outgoing particle not observed

Acknowledgements

This work has been carried out at the University of California, Berkeley, and performed under the auspices of the U.S. Department of Energy by Lawrence Livermore National Laboratory under contract DE-AC52-07NA27344 and Lawrence Berkeley National Laboratory under contract # DE-AC02-05CH11231. Funding has been provided from the US Nuclear Regulatory Commission and the US Nuclear Data Program.

M.S. Basunia, J.C. Batchelder, J.D. Bauer, L.A. Bernstein, D.L. Bleuel, J.A. Brown, B.L. Goldblum, K.P. Harrig, L. Kirsch, T. Laplace, E.F. Matthews, M.A. Unzueta, A.S. Voyles

Thanks!

Berkeley
UNIVERSITY OF CALIFORNIA